Quantitative theory of transport in vortex matter of type-II superconductors in the presence of random pinning

B. Rosenstein and V. Zhuravlev
National Center for Theoretical Sciences and Electrophysics Department, National Chiao Tung University, Hsinchu 30050, Taiwan, Republic of China

(Received 27 January 2007; revised manuscript received 24 April 2007; published 17 July 2007)

We quantitatively describe the competition between interactions, thermal fluctuations, and random quenched disorder using the dynamical Martin-Siggia-Rose approach [Phys. Rev. A **8**, 423 (1973)] to the Ginzburg-Landau model of the vortex matter. The approach first used by Dorsey *et al.* [Phys. Rev. B **45**, 523 (1992)] to describe the linear response far from H_{c1} is generalized to include both pinning and finite voltage. It allows one to calculate the non-Ohmic *I-V* curve, thereby extending the theory beyond the linear response. The static flux line lattice in type-II superconductors undergoes a transition into three disordered phases: the vortex liquid (not pinned), the homogeneous vortex glass (pinned, if one disregards an exponentially small creep at finite temperatures), and the crystalline Bragg glass (pinned) due to both thermal fluctuations and disorder. The location of the glass transition line in the homogeneous phase is determined and compared to experiments. The line is clearly different from both the melting line and the second peak line describing the translational and rotational symmetry breaking at high and low temperatures, respectively. Time correlation and response functions of the order parameter as functions of the time difference are calculated in both the liquid and the amorphous homogeneous phases. They determine the relaxation properties of the vortex matter due to the combined effect of pinning and thermal fluctuation. We calculate the critical current as a function of magnetic field and temperature in the homogeneous phase. The surface in the *J-B-T* space defined by this function separates between a dissipative moving vortex matter regime and vortex glass. A quantitative theory of the peak effect, qualitatively different from the conventional one due to Pippard [C. Tang, X. Ling, S. Bhattacharya, and P. M. Chaikin, Europhys. Lett. **35**, 597 (1996); A. B. Pippard, Philos. Mag. **19**, 217 (1969); A. I. Larkin and Yu. N. Ovchinnikov, J. Low Temp. Phys. **34**, 409 (1978)], is proposed.

DOI: 10.1103/PhysRevB.76.014507 PACS number(s): 74.40.+k, 74.25.Ha, 74.25.Dw

I. INTRODUCTION

In type-II superconductors for which the penetration depth λ exceeds the correlation length ξ, the magnetic field penetrates the sample in the form of Abrikosov vortices which strongly interact, thereby creating an elastic "vortex matter." Impurities always present in a sample lead to inhomogeneities both on the microscopic scale (described by the electron's mean free path) and the mesoscopic scale (pinning), which greatly affect the thermodynamic and, especially, dynamic properties of the vortex matter. When disorder is strong enough, it pins the vortex matter, resulting in dissipationless persistent current, thereby recovering an original defining property of superconductor. In addition, thermal fluctuations also significantly influence the vortex matter, either directly by melting the vortex lattice into a vortex liquid or by changing the efficiency of the disorder (thermal depinning). They are especially important in high T_c superconductors. As a result of a delicate interplay between disorder, interactions, and thermal fluctuations, even the static *H-T* phase diagram of high T_c superconductors is very complex and is still far from being reliably determined.

Once electric current J is injected into a sample, one is faced with the problem of describing the dynamical phase diagram, which should be drawn in the three dimensional space *T-H-J*. This makes the analysis essentially more complicated, especially if one intends to study it beyond linear response. Generally, there are two phases: the pinned phase, in which the vortices are pinned and thus the resistivity vanishes (perfect superconductivity exists), and the unpinned phase, in which vortices can move due to Lorentz force and thus a finite resistivity appears. The transition surface is determined by the critical current as function of magnetic field H and temperature T. When the critical current vanishes, the intersection of the surface with the *H-T* plane gives the "static" irreversibility line.

Theoretically, the problem of the vortex matter subject to both thermal fluctuations and disorder has a long history. Two major simplifications are generally made. In the majority of the works, the vortex matter is considered as an array of elastic lines.[2] This (London) approximation is generally valid far from the higher critical field H_{c2}, when the vortex density is low. An alternative simplification to the vortex matter is valid far enough from the lower critical field H_{c1}. At high vortex densities, magnetic fields of many vortices overlap and the resulting magnetic inductance is nearly homogeneous. It is usually supplemented by the so-called lowest Landau level (LLL) approximation.[3,4] The original idea of the vortex glass[5] and the continuous glass transition exhibiting the glass scaling of conductivity in statics appeared early in the framework of the frustrated *XY* model.[6] The model was studied by the renormalization group and the variational methods, and has been extensively simulated numerically.[7,8] In analogy to the theory of spin glasses, in this model the replica symmetry is broken when crossing the glass transition line. The frustrated *XY* model ran into several problems. For finite penetration depth, it has no transition[9] and, moreover, there was a difficulty in explaining sharp

Bragg peaks observed in the experiments at low magnetic fields. To address the last problem, another simplified model had been proven to be more convenient: the elastic medium approach to a collection of interacting linelike objects subject to both the pinning potential and the thermal bath. The resulting theory was treated using the Gaussian approximation[10,11] and renormalization group.[6] The original problem of the very fast destruction of the vortex lattice by disorder was solved with the vortex matter being in the replica symmetry broken phase for dimensionality $2<D<4$, and it was termed "Bragg glass." In $D=2$, there exists discrete replica symmetry broken transition. It is possible to address the problem of dynamics in the presence of thermal fluctuation using an approach in which one directly simulates the interacting line-like objects subject to both the pinning potential and the thermal bath Langevin force.[12]

A vast majority of theoretical works deal with the linear response and cannot address the flux dynamics at finite currents. The *I-V* curves of the flux flow are very nonlinear. However, one should be very cautious in interpreting the experimental results since they generally do not distinguish between the bulk and the edge effects. In several experiments in which the bulk was isolated (either by Corbino geometry[13] or by varying the width of the sample[14]), one finds that the bulk *I-V* has a structure simpler than the commonly accepted nonlinear form. It is important to achieve a theoretical understanding of both the bulk and edge contributions in the region of the magnetic phase diagram in which these experiments on $NbSe_2$ were performed. Very often the flux dynamics is investigated in the London limit with widely separated vortices, so that one can model them as an array of line-like thin objects interacting pairwise. The motion in the presence of disorder looks like a rather chaotic advance in channels, with sudden hops between pinning centers and occasional avalanches. This picture cannot be directly applied in situations when magnetic field of vortices overlap, creating a homogeneous magnetic field. Still, the core regions might exhibit this type of behavior. Moreover, the connection between the qualitative description of the motion and the resulting *I-V* curves is not clear at present.

In this paper, we investigate the (bulk) dynamics of the vortex matter beyond linear response using the disordered Ginzburg-Landau model. In statics, the replica method of handling disorder in the framework of LLL Ginzburg-Landau (GL) model was utilized in both three dimensions and two dimensions[15,16] to obtain the irreversibility line along with other properties of the disordered vortex matter. The irreversibility lines of YBCO and a two-dimensional (2D) organic superconductor were found to be in good agreement with experiment.[16] Tesanovic and Herbut used supersymmetry (for columnar defects in layered materials).[17] Dynamics in the presence of thermal fluctuations and disorder is phenomenologically described using the time dependent Ginzburg-Landau (TDGL) model, in which the coefficients have random components.[2,18] Such an attempt was made by Dorsey *et al.*[1] in the homogeneous (liquid) phase using a dynamic Martin-Siggia-Rose (MSR) formalism.[19,20] They obtained the irreversibility line and formulated the linear response theory of the vortex matter.

The main purpose of this paper is to study the dynamics of three-dimensional vortex matter beyond linear response using the dynamical approach[1] within the TDGL model *at finite electric field*. In strongly type-II superconductors (for which the Ginzburg-Landau ratio $\kappa=\lambda/\xi$ is large), magnetic and electric fields inside the superconductor are homogeneous over a wide range of parameters. As mentioned above, high homogeneity of magnetic field in the mixed state originates from superposition of many $(\tilde{B}/H_{c1}\gg 1)$ vortices. The same argument is valid for an electric field which arises due to vortex motion. Indeed, the electric field is related by Lorentz transformation to the homogeneous magnetic field appearing in the frame moving with vortices. Linear response, namely, conductivity in the limit of zero current, is typically obtained using the Kubo formula.[1,21–23] A theory with a finite electric field allows one to obtain the *I-V* curve beyond the linear response. Finite electric fields without disorder have been considered within the framework of TDGL in Refs. 4, 21, and 24.

Complex motion of vortex matter featuring mesoscopic avalanches, channels, and islands of pinned flux described above, which might exist, are not probed directly in our method of averaging over the white noise disorder. Analytically, one preforms the disorder average of conductivity and magnetization, and does not directly see the picture above. To get a glimpse into the dynamics, time dependent correlation functions are calculated. We study the dynamic correlation function $C(\mathbf{r},\tau,\mathbf{r}',\tau')$ and the response functions $R(\mathbf{r},\tau,\mathbf{r}',\tau')$ (averaged over disorder and thermal fluctuations) of the order parameter ψ within an appropriately generalized Gaussian approximation in both the flux flow and the pinned phases. We consider the stationary case only,[1] namely, when the correlation function depends on the time difference and is therefore characterized by the spectrum C_ω. The critical surface $T^g(H,J)$ in the three-dimensional space *T-H-J*, separating the pinned and unpinned phases, is obtained as a surface at which $C_\omega\to\infty$ for $\omega\to 0$. Above this surface, the real space correlator decays exponentially, while below it is a constant at large time scales. The constant is proportional to the Edwards-Anderson order parameter characterizing transition to a glassy state.[25] Approaching criticality in the parameter space $T\to T^g$, various quantities diverge powerwise in $(T-T^g)$, with critical exponents calculated in mean field. The static glass transition line, namely, the line at zero electric field, coincides with the one obtained using the replica method.[16] A relation between the dynamical and replica methods, which is important for understanding the nature of any glass transition, is discussed.

We show that the leading contribution to conductivity near the glass line comes from the first Landau level rather than from the LLL. The conductivity diverges on the static glass line. This has important physical consequences. It is well known that within LLL both magnetization and conductivity are proportional to the superfluid density $|\psi|^2$. Magnetization is generally proportional to the superfluid density in the first order in $1/\kappa^2$ (see Ref. 26), while for arbitrary LLL configuration ψ, the electric current can be written as $\mathbf{J}\propto(\hat{\mathbf{z}}\times\nabla)|\psi|^2$. This relation does not hold for higher Landau levels (LLs). Experimentally, however, while magnetization is continuous across the line, the conductivity diverges. This is known to happen in a wide range of materials and param-

eters. Compare, for example, a recent experiment[27] on magnetization in BSCCO and an earlier transport measurement in the same material and the same range of parameters.[28] The fact that near the glass line contribution from higher LL (HLL) takes over removes this difficulty of the LLL theory. The exponentially small vortex creep is not included (it corresponds to instanton contribution in the formulation adopted), and therefore, is not general in this respect.

The main result of the present paper is the calculation of the *I-V* curves in a wide range of parameters. The *I-V* looks often as a shifted straight line, rather different from the smooth power-like behavior seen in many experiments. However, as mentioned above, it is consistent with recent measurements in which the edge contribution was minimized.[13,14,29] In addition, we provide an alternative theory of the peak effect in the critical current. A sharp increase of the critical current is not considered as gradual, due to softening of the vortex lattice before melting, but rather an abrupt jump into the homogeneous vortex glass state, in which we obtain large current diminishing fast while approaching the glass line.

The paper is organized as follows. The disordered TDGL model at a constant electric field is defined in Sec. II. The Martin-Siggia-Rose formalism is applied to it using the basis of Landau levels in electric field. In Sec. III, we briefly describe a variant of the Gaussian approximation functional integral method[30,31] and apply it to the MSR action for the LLL sector. We find the dynamical glass transition surface and calculate various critical exponents. The stationary correlations in the pinned phase are also found. It is shown in Sec. IV that the main contribution to the current near the glass transition line comes from higher Landau levels, and their leading contribution is calculated. The rest of the paper deals with applications of the obtained general results to experiments. The irreversibility line and the *I-V* curves are considered in Sec. V, while the critical current and the theory of the peak effect are discussed in Sec. VI. A brief discussion of the applicability of the theory and conclusions are the subjects of Sec. VII.

II. TIME DEPENDENT GL MODEL IN THE PRESENCE OF BOTH DISORDER AND THERMAL FLUCTUATIONS

A. Basic equations and assumptions

Our starting point is the TDGL equation[26] in the presence of thermal fluctuations, which on the mesoscopic scale are represented by a (complex) white noise[21,24] ζ:

$$\frac{\hbar^2\gamma}{4m^*}D_\tau\psi = -\frac{\delta}{\delta\psi^*}F + \zeta, \tag{1}$$

where m^* is the effective mass of the Cooper pair. The covariant time derivative is $D_\tau \equiv \frac{\partial}{\partial\tau} + \frac{ie^*}{\hbar}\Phi$, where Φ is the scalar electric potential describing the driving force in a purely dissipative dynamics. We assume that the charge of the Cooper pairs is negative $-e^*$, with positive $e^*=2e$. The inverse diffusion constant $\gamma/2$ controlling the time scale of dynamical processes via dissipation is real, although a small imaginary (Hall) part is generally present.[32] The variance of the thermal noise ζ determines the temperature $T=tT_c$:

$$\langle\zeta(\mathbf{r},\tau)\zeta^*(\mathbf{r}',\tau')\rangle = \delta(\tau-\tau')\delta(\mathbf{r}-\mathbf{r}')\frac{\hbar^2\gamma}{2m^*}T. \tag{2}$$

The static GL free energy including the ΔT_c disorder[1,2] is

$$F = \int d^3r\left[\frac{\hbar^2}{2m^*}\left|\left(\nabla + \frac{ie^*}{\hbar c}\boldsymbol{A}\right)\psi\right|^2 + \frac{\hbar^2}{2m_c^*}|\partial_z\psi|^2 - \alpha T_c(1-t)[1+U(\mathbf{r})]|\psi|^2 + \frac{b'}{2}|\psi|^4\right]. \tag{3}$$

The random component of T_c, $U(\mathbf{r})$, will be modeled by a white noise characterized by variance depending on the pinning:

$$\overline{U(\mathbf{r})U(\mathbf{r}')} = \delta(\mathbf{r}-\mathbf{r}')\xi^2\xi_z n_p. \tag{4}$$

The dimensionless pinning strength n_p is proportional to the density of pinning centers in units of the coherence volume $\xi^2\xi_z$, where $\xi_z=\gamma_a\xi$ with anisotropy parameter $\gamma_a=\sqrt{\frac{m^*}{m_c^*}}$. We neglect possible random components of other coefficients in TDGL. These might lead to important physical consequences and were considered using replica formalism in statics in Ref. 16. The space covariant derivative $\boldsymbol{D}\equiv\nabla+\frac{ie^*}{\hbar c}\boldsymbol{A}$, describes magnetic field, and the coefficients are related to the coherence length and the magnetic penetration depth λ via $\alpha T_c=\frac{\hbar^2}{2m^*\xi^2}$ and $b'=\frac{2\pi\hbar^2\lambda^2e^{*2}}{\xi^2c^2m^{*2}}$. The TDGL equations, therefore, can be written in a form

$$\hat{L}\psi = \alpha T_c(1-t)U\psi - b'|\psi|^2\psi + \zeta, \tag{5}$$

where a (non-Hermitian) linear operator is defined by

$$\hat{L} \equiv \frac{\hbar^2\gamma}{4m^*}D_\tau - \frac{\hbar^2}{2m^*}\boldsymbol{D}^2 - \frac{\hbar^2}{2m_c^*}\partial_z^2 - \alpha T_c(1-t). \tag{6}$$

We make several assumptions (identical to those made in Ref. 21 and major parts of Ref. 4) to simplify the problem. As was discussed in the Introduction, in strongly type-II superconductors, $\kappa=\lambda/\xi\gg1$; magnetic and electric fields are very homogeneous since fields of vortices overlap. Therefore the Maxwell type equations for electromagnetic field are not considered. The axes are chosen in such a way that the magnetic and electric fields are oriented along the negative z direction and the negative y direction, respectively. The vortices are moving along the positive x direction due to the Lorentz force. The electric and magnetic fields $\boldsymbol{E}=-\nabla\Phi-\frac{\partial}{\partial t}\boldsymbol{A}$; $\boldsymbol{B}=\nabla\times\boldsymbol{A}$ are written in the Landau gauge, with the vector potential $\boldsymbol{A}=(By,0,0)$ and the scalar potential $\Phi=Ey$, respectively. Temperatures, currents, and magnetic fields should be close "enough" to the dynamical phase transition line $H_{c2}(T,E)$ in order to apply the GL approach based on an assumption that the order parameter ψ is small.

B. Martin-Siggia-Rose formalism for TDGL model

A Langevin type dynamics can be formulated as a functional problem with the dynamical "partition function," de-

fined by the MSR functional integral[19] over the order parameter ψ and an additional "ghost" field[33] ϕ. The ghost field allows exact integration over the white noise ζ. As was noticed by Sompolinsky and Zippelius,[20] who considered a similar model in the context of the spin glass theory, this allows one to exactly average over disorder by performing a Gaussian integration over the random field $U(x)$ correlated according to Eq. (4) without invoking the replica trick:

$$Z = \int D\psi^* D\psi D\phi^* D\phi \exp\{-\mathcal{A}_{MSR}[\psi,\phi]\}. \tag{7}$$

Since (a rather nontrivial) derivation is closely analogous to the one presented in detail in Ref. 20, with certain aspects further clarified in Ref. 34, we just presented the resulting action $\mathcal{A}_{MSR}[\psi,\phi]$. This choice is more convenient for performing Gaussian approximation and does not lead to any mathematical complications.

The functional approach enables us to calculate both the dynamics correlators and response function of the system in close analogy to the calculation of the static correlators in statistical physics. For example, the dynamical correlator and the response function are

$$C(\mathbf{r},\tau,\mathbf{r}',\tau') = \langle \psi_{\mathbf{r}}(\tau)\psi^*_{\mathbf{r}'}(\tau')\rangle = Z^{-1}\int D\psi^* D\psi D\phi^* D\phi \psi_{\mathbf{r}}(\tau) \times \psi^*_{\mathbf{r}'}(\tau')\exp\{-\mathcal{A}_{MSR}[\psi,\phi]\}, \tag{8}$$

$$R(\mathbf{r},\tau,\mathbf{r}',\tau') = \langle \psi_{\mathbf{r}}(\tau)\phi^*_{\mathbf{r}'}(\tau')\rangle = Z^{-1}\int D\psi^* D\psi D\phi^* D\phi \psi_{\mathbf{r}}(\tau) \times \phi^*_{\mathbf{r}'}(\tau')\exp\{-\mathcal{A}_{MSR}[\psi,\phi]\}. \tag{9}$$

From now on, $\langle\cdots\rangle$ will denote both the thermal and disorder averages. The dimensionless "action" contains a quadratic part and two quartic parts (omitting certain counterterms that will be mentioned below in Sec. III B),

$$\mathcal{A}_{free} = \frac{1}{T\gamma\xi^2}\int_{\mathbf{r},\tau}\{\phi^*_{\mathbf{r}}(\tau)\hat{L}\psi_{\mathbf{r}}(\tau) + \text{c.c.}\} - \frac{\hbar^2}{2Tm^*\gamma\xi^4}\int_{\mathbf{r},\tau}\phi_{\mathbf{r}}(\tau)\phi^*_{\mathbf{r}}(\tau) - \frac{4b' l^2\xi_z}{\gamma\xi^2\alpha T_c}\int_{\mathbf{r},\tau}\psi_{\mathbf{r}}(\tau)\psi^*_{\mathbf{r}}(\tau), \tag{10}$$

$$\mathcal{A}_{dis} = -\frac{2\xi_z}{\gamma^2\xi^2}n_p\left[\frac{\alpha(1-t)}{t}\right]^2\int_{\mathbf{r},\tau,\sigma}[\phi^*_{\mathbf{r}}(\tau)\psi_{\mathbf{r}}(\tau) + \phi_{\mathbf{r}}(\tau)\psi^*_{\mathbf{r}}(\tau)] \times [\phi^*_{\mathbf{r}}(\sigma)\psi_{\mathbf{r}}(\sigma) + \phi_{\mathbf{r}}(\sigma)\psi^*_{\mathbf{r}}(\sigma)], \tag{11}$$

$$\mathcal{A}_{int} = \frac{b'}{T\gamma\xi^2}\int_{\mathbf{r},\tau}\psi_{\mathbf{r}}(\tau)\psi^*_{\mathbf{r}}(\tau)[\phi^*_{\mathbf{r}}(\tau)\psi_{\mathbf{r}}(\tau) + \phi_{\mathbf{r}}(\tau)\psi^*_{\mathbf{r}}(\tau)], \tag{12}$$

where the operator $\hat{L}$ was defined in Eq. (6). The second term in Eq. (10) appears due to thermal noise averaging, while the last one represents a functional Jacobian arising from normalization of the ghost field integration.[19,34] The two quartic parts describe the disorder and the interactions, respectively.

In the theoretical part of this paper, we will use appropriate units of time $\tau' = \tau/\tau_{GL}$ with characteristic GL time scale $\tau_{GL} = \gamma\xi^2$ and coordinates $x' = x/l$, $y' = y/l$, $z' = z/\xi_z$, where magnetic length is $l = \xi b^{-1/2}$ with $b = B/B_{c2}$. It is convenient to combine the fields in a dimensionless two component column

$$\Psi = \left(\frac{\alpha l^2\xi_z}{t}\right)^{1/2}\begin{pmatrix}\psi\\ \phi\end{pmatrix},$$

in terms of which the action takes the form

$$\mathcal{A}_{free} = \int_{\mathbf{r},\tau}\Psi^*_{\mathbf{r}}(\tau)D^{-1}\Psi_{\mathbf{r}}(\tau),$$

$$\mathcal{A}_{dis} = -ng\int_{\mathbf{r}}\left[\int_{\tau}\Psi^*_{\mathbf{r}}(\tau)\sigma_x\Psi_{\mathbf{r}}(\tau)\right]^2,$$

$$\mathcal{A}_{int} = \frac{g}{2}\int_{\mathbf{r}\tau}[\Psi^*_{\mathbf{r}}(\tau)\sigma_{\uparrow}\Psi_{\mathbf{r}}(\tau)][\Psi^*_{\mathbf{r}}(\tau)\sigma_x\Psi_{\mathbf{r}}(\tau)]. \tag{13}$$

Here, we introduced two dimensionless couplings

$$n = \frac{n_p}{4\pi\sqrt{2Gi}}\frac{(1-t)^2}{t}, \tag{14}$$

characterizing the relative strength of disorder compared to interactions, and

$$g = 8\pi bt\sqrt{2Gi}, \tag{15}$$

characterizing the interactions compared to thermal fluctuations with $\sqrt{2Gi} = \frac{b'}{4\pi\alpha^2 T_c\xi^2\xi_z}$. The inverse propagator matrix is

$$D^{-1} = \begin{pmatrix}-2g & \hat{L}^+\\ \hat{L} & -1\end{pmatrix}, \tag{16}$$

where the operator $\hat{L}$ of Eq. (6) has the form

$$\hat{L} = \frac{1}{2}(\partial_\tau + 4ibvy) - b[(\partial_x - iy)^2 + \partial_y^2] - \partial_z{}^2 - (1-t), \tag{17}$$

with velocity of fluxons

$$v = \frac{e^*\gamma El^3}{4\hbar} \tag{18}$$

given in units of c. We make use of Pauli matrices σ_x, σ_y, σ_z, and $\sigma_{\uparrow,\downarrow} = \frac{1}{2}(1 \pm \sigma_z)$.

Since the spectrum of the operator $\hat{L}$ is discrete (the Landau quantization), in a certain range of parameters, one can significantly simplify the problem by considering the "low energy" states only. It is therefore advantageous to reexpress the model in the Landau level basis.

C. Landau level basis in the presence of electric field

The moving Landau harmonics are solutions of linearized time dependent GL equation in the presence of electric field.

Mathematically, we define them as the right eigenfunctions of the operator $\hat{L}$, Eq. (17), with eigenvalues L_{Nk,k_z}: $\hat{L}(e^{-i\omega\tau}\varphi_{Nk,k_z})=L_{Nk,k_z}(e^{-i\omega\tau}\varphi_{Nk,k_z})$, where

$$\varphi_{Nk,k_z}=\frac{1}{\sqrt{2^N N!\,\pi^{1/2}}}e^{-v^2/2}H_N(y-k+iv)\exp[ik_z z]\times\exp[ikx]\exp\left[-\frac{1}{2}(y-k+iv)^2\right], \tag{19}$$

and $H_N(y)$ are Hermit polynomials. The basis functions are normalized as

$$\int_{\mathbf{r}}\bar{\varphi}_{N\mathbf{k}'}(\mathbf{r})\varphi_{M\mathbf{k}}(\mathbf{r})=(2\pi)^2\delta_{\mathbf{k}'\mathbf{k}}\delta_{N,M} \tag{20}$$

and $\delta_{\mathbf{k}'\mathbf{k}}$ is the 2D δ function with $\mathbf{k}=\{k,k_z\}$. Since the operator is not Hermitian, they are different from the left eigenfunctions $\bar{\varphi}_{Nk,k_z}$ defined as $\hat{L}^{\dagger}(e^{i\omega\tau}\bar{\varphi}_{Nk,k_z})=L^{*}_{Nk,k_z}(e^{i\omega\tau}\bar{\varphi}_{Nk,k_z})$, see Ref. 24.

The order parameter and the ghost fields are expanded, therefore, via the moving Landau harmonics as

$$\Psi_{\mathbf{r}}(\tau)=\frac{1}{(2\pi)^{3/2}}\sum_{N=0}\int_{\omega\mathbf{k}}e^{-i\omega\tau}\varphi_{N\mathbf{k}}(\mathbf{r})\Psi_{N\mathbf{k},\omega}. \tag{21}$$

We will use in Sec. III the LLL subspace, although higher levels will be necessary for the calculation of supercurrent and will be considered in Sec. IV. It will be convenient to separate the presumably more important LLL subspace from the rest, the HLL part:

$$\Psi_{\mathbf{r}}(\tau)=\Phi_{\mathbf{r}}(\tau)+\Theta_{\mathbf{r}}(\tau), \tag{22}$$

where $\Phi_{\mathbf{k},\omega}\equiv\Psi_{0\mathbf{k},\omega}$ and $\Theta_{\mathbf{k},\omega}\equiv\Sigma_{N=1}\Psi_{N\mathbf{k},\omega}$. As will become clear in Sec. IV, it will be sufficient for our purposes to consider effects up to first order in $\Theta_{\mathbf{r}}(\tau)$, and now, we concentrate on the LLL sector.

In the LLL sector, the quadratic part of the action takes the form

$$\mathcal{A}_{free}=\int_{\mathbf{k},\omega}\Phi^{*}_{\mathbf{k},\omega}D^{-1}_{\mathbf{k}\omega}\Phi_{\mathbf{k},\omega},$$

$$D^{-1}_{\mathbf{k}\omega}=\begin{pmatrix}-2g & \frac{i\omega'}{2}+k_z^2+2a_h\\ \frac{-i\omega'}{2}+k_z^2+2a_h & -1\end{pmatrix}, \tag{23}$$

where $\omega'=\omega-4bvk$ and $a_h=-(1-t-b-bv^2)/2$ is the "distance" on the dynamical phase diagram from the mean field normal-superconductor transition line. The quartic terms are

$$\mathcal{A}_{dis}=-\frac{ng}{(2\pi)^{5/2}}\int_{[\mathbf{k}],\omega,\nu}\delta_{\mathbf{k}_1-\mathbf{k}_2+\mathbf{k}_3-\mathbf{k}_4}f_0([k])(\Phi^{*}_{\mathbf{k}_1,\omega}\sigma_x\Phi_{\mathbf{k}_2,\omega})\times(\Phi^{*}_{\mathbf{k}_3,\nu}\sigma_x\Phi_{\mathbf{k}_4,\nu}), \tag{24}$$

$$\mathcal{A}_{int}=\frac{g}{2(2\pi)^{7/2}}\int_{[\mathbf{k}],[\omega]}\delta^{\mathbf{k}_1-\mathbf{k}_2+\mathbf{k}_3-\mathbf{k}_4}_{\omega_1-\omega_2+\omega_3-\omega_4}f_0([k])(\Phi^{*}_{\mathbf{k}_1,\omega_1}\sigma_{\uparrow}\Phi_{\mathbf{k}_2,\omega_2})\times(\Phi^{*}_{\mathbf{k}_3,\omega_3}\sigma_x\Phi_{\mathbf{k}_4,\omega_4}), \tag{25}$$

where $[\mathbf{k}]$ and $[\omega]$ denote a set of all variables $\{\mathbf{k}_1,\mathbf{k}_2,\mathbf{k}_3,\mathbf{k}_4\}$ and $\{\omega_1,\omega_2,\omega_3,\omega_4\}$, respectively, and $\delta^{\mathbf{k}_1-\mathbf{k}_2+\mathbf{k}_3-\mathbf{k}_4}_{\omega_1-\omega_2+\omega_3-\omega_4}$ is a product of Dirac δ functions $\delta(\omega_1-\omega_2+\omega_3-\omega_4)\delta(\mathbf{k}_1-\mathbf{k}_2+\mathbf{k}_3-\mathbf{k}_4)$. The Gaussian damping factor $f_0([k])=\exp\left[-\frac{(k_2-k_1)^2+(k_4-k_1)^2}{2}\right]$ arises from matrix elements of four LLL functions.

III. CONSISTENT GAUSSIAN APPROXIMATION FOR THE MSR ACTION

Since the model is highly nontrivial even in the simplest cases, one has to use an approximation scheme. We utilize a method which evolved from the Gaussian variational approach to quantum mechanics, referred to here as Gaussian approximation.[31] Generally, it captures the basic physical aspects, although its precision might not be very high (perhaps similar to a dynamical mean field theory in the band structure calculations).

Since we will calculate higher correlators using well known, sometimes inconsistently, Gaussian approximation, we start with a brief description of the general method introduced in detail in Ref. 30, utilizing the so-called Gaussian effective action and "truncated" Dyson-Schwinger equations. Naively using the Hartree-Fock procedure (Wick contractions) to calculate correlators leads to several important inconsistencies. For example, approximate correlators of Goldstone bosons are not massless, contrary to the Goldstone theorem. This is crucial in calculating effects dependent on massless modes like the divergence of conductivity on the glass line. An additional advantage of this approach over the resummation of the diagram technique used in Refs. 1 and 23 (borrowed from the physics of weak localization) is that it is systematic and unambiguous, without any reference to the "large number of components" limit.

A. Gaussian effective action and correlators

The exact effective action $\mathcal{A}(\bar{\Psi},G)$ introduced by Cornwall *et al.*[35] is defined as the functional of two variational parameters, a "classical" (or shift) field

$$\bar{\Psi}_A=\langle\Psi_A\rangle=Z^{-1}\int_{\Psi,\Psi^{*}}\Psi_A\exp\{-\mathcal{A}_{MSR}[\Psi,\Psi^{*}]\} \tag{26}$$

and a two-field connected correlator

$$G_{AB}=\langle(\Psi_A-\bar{\Psi}_A)(\Psi^{*}_B-\bar{\Psi}^{*}_B)\rangle=Z^{-1}\int_{\Psi,\Psi^{*}}(\Psi_A-\bar{\Psi}_A)(\Psi^{*}_B-\bar{\Psi}^{*}_B)\exp\{-\mathcal{A}_{MSR}[\Psi,\Psi^{*}]\}. \tag{27}$$

Here, indices of the field Ψ stand for the full set of variables and parameters: $A=\{\omega,\mathbf{k},i\}$, where $i=1,2$ is the Ψ column

index. Minimization of the effective action yields the "shift" and the "gap" equations

$$\frac{\delta \mathcal{A}(\bar{\Psi},G)}{\delta \bar{\Psi}_A}=0, \quad \frac{\delta \mathcal{A}(\bar{\Psi},G)}{\delta G_{AB}}=0, \tag{28}$$

respectively.

In the Gaussian approximation, $\mathcal{A}(\bar{\Psi},G)$ is approximated (up to an unimportant constant) by

$$\mathcal{A}(\bar{\Psi},G) \simeq \mathcal{A}_G(\bar{\Psi},G)=\mathcal{A}_{free}[\bar{\Psi}]-\mathrm{Tr}\log G+\mathrm{Tr}\{D^{-1}G\} + \langle \mathcal{A}_{dis}\rangle_G+\langle \mathcal{A}_{int}\rangle_G, \tag{29}$$

where $\mathcal{A}_{free}[\bar{\Psi}]$ is the quadratic part of $\mathcal{A}_{MSR}[\bar{\Psi}]$ action in Eq. (10) and $\langle \mathcal{A}_{dis}\rangle_G$, $\langle \mathcal{A}_{int}\rangle_G$ are calculated as the Gaussian averages with the field shifted by $\bar{\Psi}$:

$$\langle O\rangle_G=\frac{\int_{\Psi,\Psi^*} O[\Psi,\Psi^*]\exp[-(\Psi^*-\bar{\Psi}^*)G^{-1}(\Psi-\bar{\Psi})]}{\int_{\Psi,\Psi^*}\exp[-(\Psi^*-\bar{\Psi}^*)G^{-1}(\Psi-\bar{\Psi})]}.$$

This allows calculation of correlators of the fields via functional differentiation with respect to the shift fields. In the rest of this section, we will solve the gap equations for the MSR action, while correlators (including the four-point functions) are considered in Sec. IV.

B. Application to the LLL model: The gap equation

The Gaussian approximation has been applied to the LLL time dependent Ginzburg-Landau model in the absence of electric field using diagram resummation in Ref. 1. Here, we use the Gaussian effective action approach leading to an identical gap equation. Assuming that the gauge (electric charge) U(1) symmetry is unbroken, the one-field averages $\langle\psi\rangle$, $\langle\phi\rangle$ and the "charged" two-field correlators like $\langle\psi\psi\rangle$ should vanish. The invariant ("neutral") two-point Green functions include the correlator $C(\mathbf{r},\tau,\mathbf{r}',\tau')\sim\langle\psi_{\mathbf{r}}(\tau)\psi^*_{\mathbf{r}'}(\tau')\rangle$, the response function $R(\mathbf{r},\tau,\mathbf{r}',\tau')\sim\langle\psi_{\mathbf{r}}(\tau)\phi^*_{\mathbf{r}'}(\tau')\rangle$, and the auxiliary field correlator $B(\mathbf{r},\tau,\mathbf{r}',\tau')\sim\langle\phi_{\mathbf{r}}(\tau)\phi^*_{\mathbf{r}'}(\tau')\rangle$ (which will vanish; see below). In a homogeneous dynamical phase (physically corresponding to a stationary flux flow), the correlators depend on the differences $\tau-\tau'$ and $\mathbf{r}'-\mathbf{r}$ only. Therefore, in the $\{\omega,\mathbf{k}\}$ space, one has

$$G_{AA'}=\delta_{\omega\omega'}\delta_{\mathbf{k}\mathbf{k}'}G_{\omega\mathbf{k}}, \quad G_{\omega\mathbf{k}}=\begin{pmatrix} C_{\omega\mathbf{k}} & R_{\omega\mathbf{k}} \\ R^*_{\omega\mathbf{k}} & B_{\omega\mathbf{k}}\end{pmatrix}, \tag{30}$$

where $\delta_{\omega\omega'}\equiv\delta_{\omega-\omega'}$ and $\delta_{\mathbf{k}\mathbf{k}'}=\delta_{\mathbf{k}-\mathbf{k}'}$ are the one- and two-dimensional Dirac delta functions $\delta(\omega-\omega')$ and $\delta(k-k')\delta(k_z-k'_z)$, respectively.

Making use of the above relation, the quartic terms in Eq. (29) become

$$\langle \mathcal{A}_{dis}\rangle_g=-\frac{ng}{(2\pi)^{5/2}}\delta_\omega\delta_{\mathbf{k}}\int_{[\mathbf{k}],[\mathbf{k}'],\omega} f_R(k'-k)\mathrm{Tr}(\sigma_x G_{\omega\mathbf{k}}\sigma_x G_{\omega\mathbf{k}'}), \tag{31}$$

$$\langle \mathcal{A}_{int}\rangle_g=\frac{g\delta_\omega\delta_{\mathbf{k}}}{2(2\pi)^{7/2}}\int_{[\mathbf{k}],[\mathbf{k}'],\omega,\nu} f_R(k'-k)[\mathrm{Tr}(\sigma_\uparrow G_{\omega\mathbf{k}}\sigma_x G_{\nu\mathbf{k}'}) + \mathrm{Tr}(\sigma_\uparrow G_{\omega\mathbf{k}})\mathrm{Tr}(\sigma_x G_{\nu\mathbf{k}'})], \tag{32}$$

where $\delta_\omega=\frac{1}{2\pi}\int_\tau$ and $\delta_{\mathbf{k}}=\frac{1}{(2\pi)^2}\int_{\mathbf{r}}$ are infinite constants, and $f_R(k)=\exp\left[-\frac{k^2}{2}\right]$ is a reduced version of the damping factor $f_0([k])$ due to the momentum conservation. In the disorder term, we omitted the Wick contractions within the curly brackets in Eq. (24), since they are canceled exactly by the disorder "counterterms" in the MSR action, see Ref. 34. Calculating the functional derivative of $\mathcal{A}_g(\bar{\Phi},G)$, the gap equation is written in a well known form

$$G^{-1}_{AB}=D^{-1}_{AB}+M_{AB}, \quad M_{AB}=\frac{\delta}{\delta G_{AB}}(\langle \mathcal{A}_{dis}\rangle_{gauss}+\langle \mathcal{A}_{int}\rangle_{gauss}).$$

Note that G_{AB} is a symmetric function with respect to transposition of all its indices. Substituting the matrix M_{AB} as a function of G_{AB} into the gap equation, we arrive at

$$G^{-1}_{\omega\mathbf{k}}=\tilde{D}^{-1}_{\omega\mathbf{k}}-\frac{2ng}{(2\pi)^{5/2}}\int_{[\mathbf{k}']} f_R(k'-k)\sigma_x G_{\omega\mathbf{k}'}\sigma_x \tag{33}$$

with

$$\tilde{D}^{-1}_{\omega\mathbf{k}}=D^{-1}_{\omega\mathbf{k}}+\frac{g}{(2\pi)^{7/2}}\int_{[\mathbf{k}'],\nu} f_R(k'-k) \times[\sigma_\uparrow \mathrm{Tr}(\sigma_x G_{\nu\mathbf{k}'})+\sigma_x \mathrm{Tr}(\sigma_\uparrow G_{\nu\mathbf{k}'})]. \tag{34}$$

Here, one clearly sees the difference between the disorder and the interaction contributions in the Gaussian approximation. The interaction term just renormalizes the quadratic term in the action, while the disorder term is both frequency and wave vector dependent. We make use of this observation to simplify the gap equation.

1. Simplification of the gap equation for response function and correlator

To allow a solution of the gap equation in a closed form, we expand correlation functions (of k') in Eqs. (33) and (34), $\sigma_x G_{\omega\mathbf{k}'}\sigma_x$ and $\sigma_\uparrow \mathrm{Tr}(\sigma_x G_{\nu\mathbf{k}'})+\sigma_x \mathrm{Tr}(\sigma_\uparrow G_{\nu\mathbf{k}'})$, near the point $k'=k$ and retain only the first two terms. The correlation function depends analytically on electric field, and the leading correction $\frac{\partial^2 G_{\nu k}}{\partial k^2}$ is proportional to the square of the electric field. Furthermore, one can neglect it due to the typical smallness of the velocity parameter [defined in Eq. (18)], $v\ll 1$. This approximation does not mean that we will not be interested in important nonanalytic nonlinearities later on. For justification of the above statement, one observes that, according to Eq. (23), the inverse propagator $D^{-1}_{\omega\mathbf{k}}$ depends only on the combination $\omega'=\omega-4bvk$ of ω and k. Since in the zero order of the expansion all the dependencies on ω

and k come from $D_{\omega\mathbf{k}}$, the exact Green function, $G_{\omega\mathbf{k}}$, also depends on ω' only and, therefore, $\frac{\partial^2 G_{\omega\mathbf{k}}}{\partial k^2} \simeq v^2 \frac{\partial^2 G_{\omega' k_z}}{\partial \omega'^2}$. Here, we have used the fact that $G_{\omega' k_z}$ and its second derivative are of the same order in v (see the solution obtained below) and are analytic. We also have solved the full equation numerically by iterations and verified that the errors are exponentially negligible. In this approximation, the gap equation is transformed into the following form (in what follows, we drop "primes" in ω' using notation $G_{\omega k_z}$ for $G_{\omega\mathbf{k}}=G_{\omega-4bvk,k_z}$):

$$G^{-1}_{\omega k_z} = \tilde{D}^{-1}_{\omega k_z} - \frac{2ng}{(2\pi)^2}\int_{k'_z} \sigma_x G_{\omega k'_z}\sigma_x, \tag{35}$$

$$\tilde{D}^{-1}_{\omega k_z} = D^{-1}_{\omega k_z} + \frac{g}{(2\pi)^3}\int_{k'_z,\nu} [\sigma_\uparrow \mathrm{Tr}(\sigma_x G_{\nu k'_z}) + \sigma_x \mathrm{Tr}(\sigma_\uparrow G_{\nu k'_z})]. \tag{36}$$

Equation (35) is satisfied for vanishing correlator of the ghost fields, $B_\omega=0$, because the Eq. (11) matrix elements in both $G^{-1}_{\omega k_z}$ and $\sigma_x G_{\omega k'_z}\sigma_x$ are proportional to B_ω as it should be generally.[34] The correspondent matrix element of $\tilde{D}^{-1}_{\omega k_z}$ is equal to zero if the following condition is valid:

$$\frac{1}{(2\pi)^3}\int_{\omega k_z} \mathrm{Tr}(\sigma_x G_{\omega k_z}) = \frac{1}{(2\pi)^3}\int_{\omega k_z} (R_{\omega k_z} + R^*_{\omega k_z}) = 2. \tag{37}$$

The above self-consistency condition should be checked for a solution of the gap equation. The dependence on momentum along the magnetic field direction z is rather trivial and will be treated first.

2. Integrating out the direction along the magnetic field

As a next step, we factor out the k_z dependence. Note that the last term in Eq. (35) and the interaction correction in $\tilde{D}^{-1}_{\omega k_z}$ are both k_z independent, so that the dependence of $G^{-1}_{\omega k_z}$ on k_z is determined, according to Eq. (23), solely by an additive k_z dependent term in $D^{-1}_{\omega k_z}$. Therefore, the solution has the form

$$\tilde{D}^{-1}_{\omega k_z} = \tilde{D}^{-1}_{\omega} + k_z^2\sigma_x, \quad G^{-1}_{\omega k_z} = G^{-1}_{\omega} + k_z^2\sigma_x, \tag{38}$$

in which a matrix valued function of one variable ω,

$$G_\omega = G_{\omega k_z=0} \equiv \begin{pmatrix} C_\omega & R_\omega \\ R^*_\omega & 0 \end{pmatrix}, \tag{39}$$

remains to be determined. In terms of elements of G_ω, the correlators integrated over k_z are given by

$$\frac{1}{\pi}\int_{k_z} G_{\omega k_z} = \sigma_x(\sigma_x G_\omega)^{1/2} = \begin{pmatrix} \dfrac{C_\omega}{R^{1/2}_\omega + R^{*1/2}_\omega} & R^{1/2}_\omega \\ R^{*1/2}_\omega & 0 \end{pmatrix}. \tag{40}$$

Substituting Eq. (38) into Eq. (35), we arrive, after integration over k_z,

$$G^{-1}_\omega = \tilde{D}^{-1}_\omega - \frac{ng}{2\pi}(\sigma_x G_\omega)^{1/2}\sigma_x, \tag{41}$$

at a cubic equation for a matrix variable $(\sigma_x G_\omega)^{1/2}$:

$$\frac{ng}{2\pi}(\sigma_x G_\omega)^{3/2} - A_\omega(\sigma_x G_\omega) + 1 = 0. \tag{42}$$

Here, the matrix

$$A_\omega = \tilde{D}^{-1}_\omega \sigma_x = \begin{pmatrix} i\dfrac{\omega}{2} + 2a_{int} & 0 \\ -1 & -i\dfrac{\omega}{2} + 2a_{int} \end{pmatrix},$$

$$a_{int} = a_h + \frac{g}{(2\pi)^3}\int_{\omega k_z} C_{\omega k_z}, \tag{43}$$

as well as $\sigma_x G_\omega$ and its powers in Eq. (42) are triangular matrices with zero [12] component. The [22] component of Eq. (42),

$$\frac{ng}{2\pi}R^{3/2}_\omega - \left(-i\frac{\omega}{2} + 2a_{int}\right)R_\omega + 1 = 0, \tag{44}$$

determines R_ω in terms of a_{int}, while the [21] component expresses C_ω via R_ω:

$$C_\omega = \frac{R_\omega R^*_\omega (R^{1/2}_\omega + R^{*1/2}_\omega)}{R^{1/2}_\omega + R^{*1/2}_\omega - \dfrac{ng}{2\pi}R_\omega R^*_\omega}. \tag{45}$$

The remaining [11] component yields the complex conjugate equation to the first one, Eq. (44). The constant a_{int}, in turn, depends exclusively on C_ω, so the loop closes. It is important to emphasize that the only effect of interaction in the gap equations (44) and (45) is to renormalize a_h upward to a_{int}. This allows one to consider the excitations of the vortex liquid for negative a_h since a_{int} is always positive.[3]

It is convenient to rescale the correlation functions as

$$g_{\omega k_z} \equiv \begin{pmatrix} c_{\omega k_z} & \rho_{\omega k_z} \\ \rho^*_{\omega k_z} & 0 \end{pmatrix} = \left(\frac{g}{8\pi}\right)^{2/3} G_{\omega k_z},$$

$$c_\omega = \left(\frac{g}{8\pi}\right)^{2/3} C_\omega, \quad \rho_\omega = \left(\frac{g}{8\pi}\right)^{2/3} R_\omega, \tag{46}$$

and define a new parameter, the conventional LLL scaled temperature[3,17] $a_T=2(8\pi/g)^{2/3}a_h$. In this variable, the gap equation for the correlation functions is reduced to

$$4r\rho^{3/2}_\omega - \left[a_T + \frac{4}{2\pi}\int_\nu \frac{c_\nu}{\rho^{1/2}_\nu + \rho^{*1/2}_\nu} - \frac{i}{2}\left(\frac{8\pi}{g}\right)^{2/3}\omega\right]\rho_\omega + 1 = 0, \tag{47}$$

$$c_\omega = \left(\frac{8\pi}{g}\right)^{2/3} \frac{\rho^*_\omega \rho_\omega (\rho^{1/2}_\omega + \rho^{*1/2}_\omega)}{\rho^{1/2}_\omega + \rho^{*1/2}_\omega - 4n\rho^*_\omega\rho_\omega}, \tag{48}$$

where g was defined in Eq. (15). In a certain range of the parameters, namely, in the "liquid" phase in which disorder

does not alter the vacuum structure significantly, the solution can be found assuming the validity of the dissipation-fluctuation theorem (DFT), which subsequently can be checked by substitution back into the gap equation. In a more complicated "glass" phase, the DFT is violated and a solution is found later using a different method.

C. Solution of the gap equations, the glass line, and critical exponents

1. Unpinned phase

Let us assume the validity of the DFT,

$$\int_v C_{q_z \nu} = 2\pi R_{q_z \omega=0},$$

which, after integration over q_z, yields

$$\frac{1}{2\pi}\int_\nu \frac{c_\nu}{\rho_\nu^{1/2} + \rho_\nu^{*1/2}} = \rho_0^{1/2}, \tag{49}$$

with ρ_0 defined as $\rho_0 \equiv \rho_{\omega=0}$. Combining the above relation with Eq. (47) at $\omega=0$, one obtains a cubic equation for ρ_0 (which is a function of external parameters r and a_T):

$$-4(1-n)\rho_0^{3/2} - a_T\rho_0 + 1 = 0. \tag{50}$$

The solution is

$$\rho_0(a_T) = -\frac{a_T + a_T^2 d^{-1/3} + d^{1/3}}{12(1-n)^{4/3}},$$

$$d = a_T^3 + 12(1-n)\sqrt{324(1-n)^2 - 3a_T^3} - 216(1-n)^2. \tag{51}$$

In what follows, we will need its asymptotic form for large negative a_T in the clean limit, $n \to 0$,

$$\rho_0^{1/2} = -\frac{a_T}{4}. \tag{52}$$

Further, solving Eq. (50), one can substitute the solution into Eq. (47) to obtain a closed form cubic equation for the frequency dependent response function ρ_ω,

$$4n\rho_\omega^{3/2} - 4\rho_0^{1/2}\rho_\omega - a_T\left(1 - \frac{i\omega}{4a_h}\right)\rho_\omega + 1 = 0. \tag{53}$$

It should be noted that, according to Eq. (48), ρ_ω determines the correlator c_ω completing the solution of the set of the gap equations. Obviously, both the response function and the correlator can be written in an explicit form. A characteristic shape of the correlators is shown in Fig. 1. We also made use of these explicit functions for a numerical check of DFT. However, below we are mainly interested in analytic properties of the correlation functions, which can be investigated without using the explicit expressions.

The result for the integral over frequency of the correlator coincides with the static correlator calculated using the replica formalism in Gaussian approximation.[15,16] As was discussed in these papers, $n>1$ corresponds to a case in which disorder overpowers "repulsive" interaction and destabilizes the system.

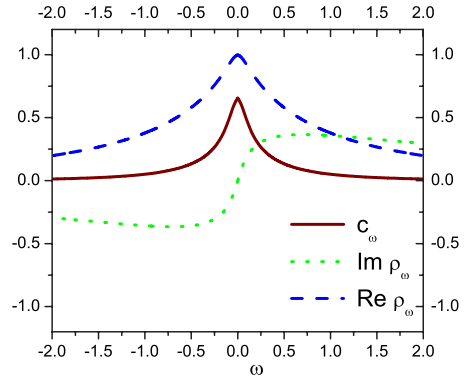

FIG. 1. (Color online) A typical form of the dimensionless correlator (the brown solid line), and the real (the blue dash line) and imaginary (green dot line) parts of the response function above the glass transition. $\Delta > 0$ are shown as a function of frequency ω.

2. Glass line and critical behavior

The critical surface in the "space" of dimensionless scaled parameters (t,b,v) is defined as a set of values of the parameters for which the correlator C_ω at $\omega=0$ diverges. The static glass line is a line on this surface for zero electric field, $v=0$. We will argue later that below this line the superconductor acquires certain "glassy" properties.

According to the gap equation, Eq. (48), the correlator $c_{\omega=0}$ becomes infinite when

$$\rho_0 = \frac{1}{(2n)^{2/3}}. \tag{54}$$

Here, ρ_0 as a function of the external parameters (r,a_T) is given by Eq. (50). Excluding ρ_0, one arrives at a simple formula for the glass surface:

$$a_T^g = (2n)^{2/3}\left(3 - \frac{2}{n}\right), \tag{55}$$

which, in terms of scaled parameters (t,b,v), is equivalent to

$$bv_g^2 = 1 - t - b + \left(\frac{ng}{4\pi}\right)^{2/3}\left(3 - \frac{2}{n}\right). \tag{56}$$

The critical velocity v_g determines the critical electric field $\mathcal{E}_g$, which destroys the glassy state, forcing vortices to move in a direction perpendicular to the field. The static glass line is described by Eq. (56) for zero electric field, $v_g=0$. This result is consistent with the one obtained using the replica method[16] in a similar Gaussian approximation.

Note that for $n=\frac{2}{3}$, the glass line coincides with the dynamic superconductor-normal metal transition line[4] $a_h=0$, whereas for a stronger disorder, $\frac{2}{3}<n<1$, it lies in the normal state, and for $n \geqslant 1$, the Gaussian effective action becomes unstable, signaling breakdown of the approximation. Similar phenomena occur in the ϕ^4 theory.[30,31] In the static $(B\text{-}T)$ phase diagram, the glass line, $B_g(T)$, begins from the point $(B=0,\ T=T_c)$, with zero derivative, $\frac{dB_g(T_c)}{dT}=0$ (see Fig.

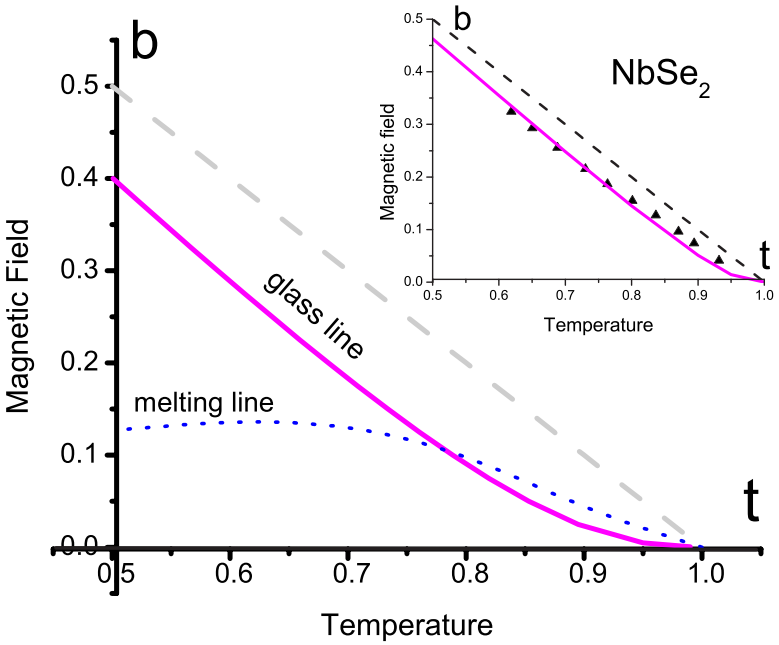

FIG. 2. (Color online) Phase diagram at high temperatures ($t=T/T_c>0.5$). The static glass transition (the magenta solid line), Eq. (96), is given for $Gi=1.25\times10^{-5}$ and $n=0.001$. A schematic behavior of the order-disorder transition is shown by a dashed line. It separates crystalline from homogeneous phases. Below the intersection with the glass line, it is the "melting line," while above it, it becomes a "peak effect line." In the inset, we present the best fit for the irreversibility line in $NbSe_2$ (see Ref. 36), with parameters given in the text.

2), and crosses $B_{c2}(T)$ line at some intermediate temperature.

The expansion of the correlation functions near the glass line in a small parameter

$$\Delta_T = a_T - a_T^g = (8\pi/g)^{2/3}\Delta \tag{57}$$

and a small frequency leads to the following critical behavior:

$$\rho_\omega = \frac{1}{(2n)^{2/3}}\left[1 - \frac{(2n)^{1/3}}{2}\sqrt{1 - i\tau_{rel}\omega}\Delta_T\right], \tag{58}$$

$$c_\omega = \frac{\tau_{rel}}{\sqrt{2}(2n)^{1/3}}\{1 + [1 + (\tau_{rel}\omega)^2]^{1/2}\}^{-1/2}\Delta_T, \tag{59}$$

where the characteristic time,

$$\tau_{rel} = \frac{8}{3\Delta_T^2}\left(\frac{2\pi}{n^2 g}\right)^{2/3}, \tag{60}$$

determines a long scale decay of the correlator.

On the critical surface, where $\Delta_T=0$ and τ_{rel} diverges, the correlator and response function,

$$\rho_\omega^g = \frac{1}{(2n)^{2/3}}\left[1 - \frac{2e^{-i\pi/4}}{\sqrt{6}}\left(\frac{4\pi}{ng}\right)^{1/3}\omega^{1/2}\right], \tag{61}$$

$$c_\omega^g = \sqrt{\frac{1}{3}}\left(\frac{8\pi}{g}\right)^{1/3}\frac{1}{n}\omega^{-1/2}, \tag{62}$$

both have a fractional power dependence on ω. One, therefore, observes criticality with exponent $\frac{1}{2}$. In the static limit near transition, the response function

$$\rho_0 = \frac{1}{(2n)^{2/3}} - \frac{\Delta_T}{2(2n)^{1/3}} \tag{63}$$

is continuous, while the correlator

$$c_0 = \frac{8}{3\sqrt{2}}\left(\frac{8\pi}{g}\right)^{2/3}\frac{1}{(2n)^{5/3}\Delta_T} \tag{64}$$

diverges with critical exponent 1.

Away from criticality, the correlator decays exponentially at large time differences, $C(\tau)\propto e^{-\pi/\tau_{rel}}$, with relaxation time determined by the singularity in the complex ω plane nearest to the origin. It, therefore, diverges with critical exponent 2.

3. Solution of the gap equation in the amorphous phase

In the glass phase, namely, when $a_T<a_T^g$, a regular solution to Eqs. (47) and (48) does not exist. This should not come as a surprise since similar phenomenon occurs in other glassy systems like spin glass.[20] In the static limit, the glassy solution takes over via continuous transition.[15,16] The same is true in dynamics. Equation (42) for C_ω component of the correlator matrix allows a more general discontinuous solution,

$$c_\omega = \left(\frac{8\pi}{g}\right)^{2/3}\frac{\rho_\omega^*\rho_\omega(\rho_\omega^{1/2} + \rho_\omega^{*1/2})}{\rho_\omega^{1/2} + \rho_\omega^{*1/2} - 4n\rho_\omega\rho_\omega^*} + \lambda\delta(\omega), \tag{65}$$

where the constant λ is the Edwards-Anderson (EA) order parameter. Indeed, in addition to a regular part (at nonzero ω) obeying the DFT, Eq. (49), which is exactly the same as on the critical line, there appears an equation for a singular (at zero ω) contribution expressing the persistent correlation $c(\tau-\tau')\to_{\tau-\tau'\to\infty}\lambda$. Substituting Eq. (54) into Eq. (47) for $\omega=0$,

$$4n\rho_0^{3/2} - \left(a_T + \frac{2}{\pi}\int_\nu \frac{c_\nu}{\rho_\nu^{1/2} + \rho_\nu^{*1/2}}\right)\rho_0 + 1 = 0,$$

one obtains

$$4n\rho_0^{3/2} - \left(a_T\rho_0 + 4\rho_0^{3/2} + \frac{\lambda}{\pi}\rho_0^{1/2}\right) + 1 = 0,$$

resulting in

$$\lambda = \frac{\pi}{(2n)^{1/3}}(a_T^g - a_T) = -\frac{\pi}{(2n)^{1/3}}\Delta_T. \tag{66}$$

The EA order parameter vanishes on the dynamical glass line and increases below it. In real space, the second term in Eq. (65) corresponds to a constant (the persistent component).[20] The expression for ρ_ω is given by a solution of Eq. (53) with $\rho_0=(2n)^{-2/3}$,

$$4n\rho_\omega^{3/2} - 4(2n)^{-1/3}\rho_\omega - a_T\left(1 - \frac{i\omega}{4a_h}\right)\rho_\omega + 1 = 0. \tag{67}$$

The regular component of the correlator in the τ space, therefore, decreases as a power $C(\tau)\propto(\tau/\tau_{GL})^{-1/2}$.

Having completed the solution of the gap equation, we now use it to calculate physical quantities other than the correlator.

IV. dc SUPERCURRENT

A. LLL contribution

In the homogeneous phase, the current density after disorder averaging is independent of both τ and $\mathbf{r}$. The average supercurrent density, therefore, is (in the geometry considered in this paper, the current flows in the y direction)

$$j_{LLL} \equiv \frac{J_{LLL}}{J'} = -\frac{i}{2}\frac{(2\pi)^3}{\mathcal{V}\mathcal{T}}\int_{\boldsymbol{\pi}} \langle \Phi_{\mathbf{r}}^*(\tau)\sigma_+\partial_y\Phi_{\mathbf{r}}(\tau)$$

$$-[\partial_y\Phi_{\mathbf{r}}^*(\tau)]\sigma_+\Phi_{\mathbf{r}}(\tau)\rangle = v\int_{\omega k_z} C_{\omega k_z}, \tag{68}$$

where $\langle\cdots\rangle$ denotes both thermal and disorder averages, and $J'=\frac{\hbar e^*}{(2\pi)^3 m^* l}\frac{t}{\alpha l^2\xi_z}=\frac{2b^{1/2}g}{(8\pi)^4}J_0$ with $J_0=\frac{e^*}{\sqrt{2}Gi}\frac{16T_c\gamma_a}{\hbar\xi^2}$, using the solutions of the gap equation and integrating over k_z. In the liquid and glass phases, the supercurrent is given by

$$j_{LLL}^{liq} = 2\pi\left(\frac{8\pi}{g}\right)^{1/3}\rho_0^{1/2}v, \tag{69}$$

$$j_{LLL}^{glass} = 2\pi\left(\frac{8\pi}{g}\right)^{1/3}\left[\frac{1}{(2n)^{1/3}} + \frac{a_T^g - a_T}{4}\right]v, \tag{70}$$

respectively. Here, ρ_0 is a solution to Eq. (50) given in Eq. (51).

Therefore, within the LLL approximation, the supercurrent is proportional to velocity times an expression analytic in velocity. Consequently, even at criticality, there exists finite conductivity $j_{LLL}^{liq}/v=2\pi\left(\frac{4\pi}{ng}\right)^{1/3}$, which is determined solely by disorder on the mesoscopic scale ng. The Ohmic behavior implies that there apparently is flux flow in both liquid and glass phases. On the glass transition, the LLL conductivity is continuous, although not a smooth function. In the glass state, we clearly see that there is no expected vortex pinning and the conductivity is finite. On the liquid side, despite the critical divergencies in correlation function discussed in Sec. III C, the conductivity does not diverge, again in contrast to experiment. The only piece of physics that the LLL approximation is able to capture is the Bardeen-Stephen flux flow conductivity far from the glass transition line and the fluctuation conductivity in normal phase.[18] In the clean limit[32] (no disorder on the mesoscopic scale), $n\to 0$ with $\rho_0^{1/2}=-\frac{a_T}{4}$ [see Eq. (52)] and one obtains

$$\sigma_{LLL} = \frac{J_{LLL}}{E} = \sigma_n\frac{1-t-b}{b}, \tag{71}$$

where σ_n is conductivity in the normal state. The full formula provides a disorder correction.

As was mentioned in the Introduction, it is quite clear physically why the LLL approximation contains the Ohmic contribution only. The current generally is proportional to a gradient of the superfluid density, which, in turn, is proportional to the electric field. The pinning effects, therefore, appear due to higher Landau levels only. We, therefore, generalize the discussion to the lowest states at which the pinning appears.

B. Higher Landau level contribution to current

The argument above leading to an Ohmic dependence of the current on electric field in LLL (confirmed by the direct calculation in the previous section) is not valid already for the first LL, $N=1$: the current is no longer a curl of the superfluid density. It is natural to assume that the HLL corrections to fields in Eq. (22) can be considered as a perturbation. Furthermore, to leading order in the perturbation, a nonzero contribution to current comes solely from the first LL (1LL):

$$j = j_{LLL} + j_{HLL},$$

$$j_{HLL} = -\frac{i}{2}\frac{(2\pi)^3}{\mathcal{V}\mathcal{T}}\int_{\mathbf{r}\tau} \langle \Phi_{\mathbf{r}}^*(\tau)\sigma_+\partial_y\Theta_{\mathbf{r}}(\tau)$$

$$-[\partial_y\Theta_{\mathbf{r}}^*(\tau)]\sigma_+\Phi_{\mathbf{r}}(\tau) + \text{c.c.}\rangle. \tag{72}$$

This is due to the fact that the operator ∂_y contains just one, raising or lowering the Landau number operator (in addition to a constant proportional to v). Thus one needs the wave function up to the first LL only,

$$\Psi_{\mathbf{r}}(\tau) = \Phi_{\mathbf{r}}(\tau) + \Theta_{\mathbf{r}}(\tau),$$

and considers it to first order in $\Theta_{\mathbf{r}}(\tau)$.

In this section, we use a simplified model compared to that used in the derivation of the gap equation in the previous section. The difference consists in the application of the steepest descent approximation (similar to that which was utilized and discussed in Sec. III B) already in the MSR action. As in Sec. III B, due to the Gaussian damping factor in quartic terms [see Eq. (24)], we neglect all the terms off-diagonal in momenta k both in the LLL and the HLL contributions:

$$\mathcal{A}_{free} = \int_{\mathbf{k},\omega} [\Phi^*_{\mathbf{k},\omega} D^{-1}_{\mathbf{k}\omega} \Phi_{\mathbf{k},\omega} + \Theta^*_{\mathbf{k},\omega} D^{-1}_{1\mathbf{k}\omega} \Theta_{\mathbf{k},\omega}],$$

$$\mathcal{A}_{dis} = -\frac{rg}{(2\pi)^2} \delta_\omega \delta_{\mathbf{k}} \int_{k,[k_z],\omega,\nu} \delta_{k_{1z}-k_{2z}+k_{3z}-k_{4z}} (\Phi^*_{k,k_{1z},\omega} \sigma_x \Phi_{k,k_{2z},\omega}) \times (\Phi^*_{k,k_{3z},\nu} \sigma_x \Phi_{k,k_{4z},\nu}) + \Delta\mathcal{A}_{dis},$$

$$\Delta\mathcal{A}_{dis} = -2^{3/2} i v \frac{rg}{(2\pi)^2} \delta_\omega \delta_{\mathbf{k}} \int_{k,[k_z],\omega,\nu} \delta_{k_{1z}-k_{2z}+k_{3z}-k_{4z}} \times [(\Phi^*_{k,k_{1z},\omega} \sigma_x \Phi_{k,k_{2z},\omega})(\Phi^*_{k,k_{3z},\nu} \sigma_x \Theta_{k,k_{4z},\nu}) - \text{c.c.}]. \tag{73}$$

Here, the inverse propagator for 1LL is

$$D^{-1}_{1\mathbf{k}\omega} = \begin{pmatrix} 0 & \frac{i\omega'}{2} + k_z^2 + 2a_h^1 \\ \frac{-i\omega'}{2} + k_z^2 + 2a_h^1 & -1 \end{pmatrix}, \tag{74}$$

where $a_h^1 = a_h + b$ is the large "mass" of the first LL excitations. The coefficient in the disorder term is chosen in such a way that the LLL gap equation obtained from this action coincides with Eq. (35). Physically, this assumption is equivalent to replacing an approximate Landau degeneracy by an exact one. In addition, we ignore the interaction term since, as was noted in Sec. III C, the interaction effects can be accounted for by renormalization of the free part of LLL action, where a_h is replaced by a_{int}.

The correction term $\Delta\mathcal{A}_{dis}$ is already proportional to the electric field via the factor v due to the fact that the integral of a product of three LLL Landau harmonics and one 1LL harmonic, Eq. (19), vanishes at zero electric field. Since $\mathcal{A}_{free}$ does not "mix" LLL with 1LL, the leading contribution to j_{HLL}, Eq. (72), will be of the second order in HLL Θ and will come from all the connected diagrams proportional to $\Delta\mathcal{A}_{dis}$.

The HLL contribution to the current from the disorder part is

$$j_{HLL} = \frac{2ng(1+2v^2)}{(2\pi)^2 a_h^1} v \int_{k[k_z]\omega\nu} \delta_{k_{1z}-k_{2z}+k_{3z}-k_{4z}} \langle (\Phi^*_{kk_{1z}\omega} \sigma_x \Phi_{kk_{2z}\omega}) \times (\Phi^*_{kk_{3z}\nu} \sigma_\uparrow \Phi_{kk_{2z}\nu}) \rangle. \tag{75}$$

One, therefore, faces a problem of a consistent calculation of the four-point Green's function. Diagrammatically, within the linear response theory, it was approximated by a resummation of the "diffusion" and "Cooperon" chains.[1] We calculate this function using a systematic approach by differentiating four times the Gaussian effective action defined in Sec. II.

Factorization of the action and of the current with respect to index k leads to proportionality of all physical quantities to the Landau degeneracy. Dropping below the index k and denoting k_z simply by k, one can express the HLL current as

$$j_{HLL} = \frac{2ng(1+2v^2)}{(2\pi)^2 a_h^1} v \sigma_{HLL}, \tag{76}$$

with the HLL contribution to the conductivity,

$$\sigma_{HLL} = \int_{\{\substack{\omega\nu \\ prqs}\}} \delta_{p+q-r-q2} \sigma_x^{u_1,v_1} \sigma_\uparrow^{u_2,v_2} \langle \Phi^{*u_1}_{p\omega} \Phi^{*u_2}_{q\nu} \Phi^{v_1}_{r\omega} \Phi^{v_2}_{s\nu} \rangle_c, \tag{77}$$

proportional to the connected part of the four-point correlation function.

C. Four-point correlators

The calculation of the four-point correlators is quite lengthy, so we first describe the general structure of the terms appearing in it. The gap equation derived in Sec. III B for Green's function $G_{AB} = \langle \Phi_A \Phi^*_B \rangle$ (where indices A and B denote the full index set of the order parameter) can be generalized to include the rest of Green's functions $F_{AB} = \langle \Phi_A \Phi_B \rangle$ and $F^*_{AB} = \langle \Phi^*_A \Phi^*_B \rangle$. In U(1) symmetric theories, like the one we consider, the last propagators are identically equal to zero due to the symmetry. However, their functional derivatives do contribute to equations for the higher vertex functions and will be necessary for our discussion.

We write the generalized gap equations in a standard form[30,31]

$$\begin{pmatrix} F^*_{B_1A_1} & G_{A_1B_1} \\ G^*_{A_1B_1} & F_{B_1A_1} \end{pmatrix} \begin{pmatrix} \frac{\delta^2 \mathcal{A}_g[\bar\Phi, G]}{\delta\bar\Phi^*_{A_1}\delta\bar\Phi^*_{A_2}}\Big|^{\text{Tr}} & \frac{\delta^2 \mathcal{A}_g[\bar\Phi, G]}{\delta\bar\Phi^*_{A_1}\delta\bar\Phi_{A_2}}\Big|^{\text{Tr}} \\ \frac{\delta^2 \mathcal{A}_g[\bar\Phi, G]}{\delta\bar\Phi_{A_1}\delta\bar\Phi^*_{A_2}}\Big|^{\text{Tr}} & \frac{\delta^2 \mathcal{A}_g[\bar\Phi, G]}{\delta\bar\Phi_{A_1}\delta\bar\Phi_{A_2}}\Big|^{\text{Tr}} \end{pmatrix} = \delta_{B_1A_2}, \tag{78}$$

where under the truncated part we understand functional derivatives of the Gaussian action $A_G[\bar\Phi, G]$, with propagators G regarded as independent of the shift fields $\bar\Phi$. Summation over repeated indices is assumed. The equations for a four-point vertex function are derived from Eq. (78) by differentiating it twice with respect to the shift field $\bar\Phi$. The field dependence of the propagators, $G[\bar\Phi]$ or $F[\bar\Phi]$, determined by the gap equation (with external "source" present), should be taken into account. It provides the "chain" parts proportional to $\frac{\delta G}{\delta\bar\Phi}$, $\frac{\delta F}{\delta\bar\Phi}$, $\frac{\delta^2 G}{\delta\bar\Phi\delta\bar\Phi}$,…. From the U(1) symmetry, one can infer that there are two nontrivial vertex contributions: the diffuson and the Cooperon parts defined by the $\frac{\delta G}{\delta\bar\Phi\delta\bar\Phi^*}$ and $\frac{\delta F}{\delta\bar\Phi\delta\bar\Phi}$ second derivatives, respectively.

The diffusion and the Cooperon equations can be obtained from Eq. (78), differentiating its (11) component with respect to $\bar\Phi_{C_2}$ and $\bar\Phi^*_{C_1}$ and differentiating the (21) component with respect to Φ_{C_2} and Φ_{C_1}:

$$\langle B_1|A_1\rangle\langle A_2|B_2\rangle \frac{\delta^2}{\delta\bar{\Phi}_{C_2}\delta\bar{\Phi}^*_{C_1}} \frac{\delta^2\mathcal{A}_g[\bar{\Phi},G]}{\delta\bar{\Phi}_{A_1}\delta\bar{\Phi}^*_{A_2}}\Bigg|^{\mathrm{Tr}} + \langle B_1|B_2;C_1|C_2\rangle = 0, \tag{79}$$

$$\frac{\delta^2}{\delta\bar{\Phi}_{C_2}\delta\bar{\Phi}_{C_1}} \frac{\delta^2\mathcal{A}_g[\bar{\Phi},G]}{\delta\bar{\Phi}^*_{A_1}\delta\bar{\Phi}^*_{A_2}}\Bigg|^{\mathrm{Tr}} \langle A_1|B_1\rangle\langle A_2|B_2\rangle + \langle|B_1B_2;|C_1C_2\rangle = 0, \tag{80}$$

where the Dirac notations,

$$\langle B_1|A_1\rangle = \langle \Phi^*_{B_1}\Phi_{A_1}\rangle,$$

$$\langle B_1|B_2;C_1|C_2\rangle = \frac{\delta G_{B_2B_1}}{\delta\bar{\Phi}_{C_2}\delta\bar{\Phi}^*_{C_1}},$$

$$\langle\,|B_1B_2;|C_1C_2\rangle = \frac{\delta F_{B_2B_1}}{\delta\bar{\Phi}_{C_2}\delta\bar{\Phi}_{C_1}},$$

have been used.

Calculating the derivatives of the Gaussian action, one obtains (specifying the full set of indices):

$$\left\langle \begin{smallmatrix} l \\ r,\nu \end{smallmatrix}\middle| \begin{smallmatrix} k \\ s,\omega \end{smallmatrix}; \begin{smallmatrix} m \\ t,\nu \end{smallmatrix}\middle| \begin{smallmatrix} n \\ u,\omega \end{smallmatrix}\right\rangle = \frac{2gn}{(2\pi)^2}\left\langle \begin{smallmatrix} l \\ r,\nu \end{smallmatrix}\middle| \begin{smallmatrix} j \\ p,\omega_2 \end{smallmatrix}\right\rangle\left\langle \begin{smallmatrix} i \\ q,\omega_1 \end{smallmatrix}\middle| \begin{smallmatrix} k \\ s,\omega \end{smallmatrix}\right\rangle \times[\delta^{q+p-q-p}\sigma_x^{i,k_1}\sigma_x^{l_1,j}\left\langle \begin{smallmatrix} l_1 \\ p,\omega_2 \end{smallmatrix}\middle| \begin{smallmatrix} k_1 \\ q,\omega_1 \end{smallmatrix}; \begin{smallmatrix} m \\ t,\nu \end{smallmatrix}\middle| \begin{smallmatrix} n \\ u,\omega \end{smallmatrix}\right\rangle + \delta^{q+t-p-u}\sigma_x^{i,j}\sigma_x^{m,n}\delta_{\omega_1-\omega_2}\delta_{\nu-\omega} + \delta^{q+t-u-p}\sigma_x^{i,n}\sigma_x^{m,j}\delta_{\omega-\omega_1}\delta_{\nu-\omega_2}], \tag{81}$$

$$\left\langle \left| \begin{smallmatrix} k \\ r,\omega \end{smallmatrix}, \begin{smallmatrix} m \\ s,\nu \end{smallmatrix};\right| \begin{smallmatrix} l \\ t,\omega \end{smallmatrix}, \begin{smallmatrix} n \\ u,\nu \end{smallmatrix}\right\rangle = \frac{2gn}{(2\pi)^2}\left\langle \begin{smallmatrix} i \\ p,\omega_1 \end{smallmatrix}\middle| \begin{smallmatrix} k \\ r,\omega \end{smallmatrix}\right\rangle\left\langle \begin{smallmatrix} j \\ q,\nu_1 \end{smallmatrix}\middle| \begin{smallmatrix} m \\ s,\nu \end{smallmatrix}\right\rangle \times[\delta^{p+q-v-w}\sigma_x^{j,g}\sigma_x^{j,h}\left\langle\left| \begin{smallmatrix} g \\ v,\omega_1 \end{smallmatrix}, \begin{smallmatrix} h \\ w,\nu_1 \end{smallmatrix};\right| \begin{smallmatrix} l \\ t,\omega \end{smallmatrix}, \begin{smallmatrix} n \\ u,\nu \end{smallmatrix}\right\rangle + \delta^{p+q-t-u}\sigma_x^{j,l}\sigma_x^{j,n}\delta_{\omega-\omega_1}\delta_{\nu-\nu_1} + \delta^{p+q-u-t}\sigma_x^{i,n}\sigma_x^{j,l}\delta_{\omega-\nu_1}\delta_{\nu-\omega_1}]. \tag{82}$$

Disconnected parts do not contribute, since they cancel with corresponding terms in action, which were discarded in Eq. (31), as we have mentioned in Sec. III A. The translational invariance allows one to define the reduced diffusion and Cooperon functions:

$$\left\langle \begin{smallmatrix} l \\ p,\nu \end{smallmatrix}\middle| \begin{smallmatrix} k \\ q,\omega \end{smallmatrix}\right\rangle = \delta^{q-p}_{\omega-\nu}G^{k,l}_{p,\nu},$$

$$\left\langle \begin{smallmatrix} l \\ r,\nu \end{smallmatrix}\middle| \begin{smallmatrix} k \\ s,\omega \end{smallmatrix}; \begin{smallmatrix} n \\ q,\nu \end{smallmatrix}\middle| \begin{smallmatrix} m \\ p,\omega \end{smallmatrix}\right\rangle = \delta_0\delta^{r-s-p+q}_{\omega-\nu}Q^{l,k;n,m}_{(r,s;q)\omega},$$

$$\left\langle\left| \begin{smallmatrix} k \\ q,\omega \end{smallmatrix}, \begin{smallmatrix} m \\ p,\nu \end{smallmatrix};\right| \begin{smallmatrix} l \\ r,\omega \end{smallmatrix}, \begin{smallmatrix} n \\ s,\nu \end{smallmatrix}\right\rangle = \delta_0\delta^{q+p-r-s}_{\omega-\nu}K^{k,m;l,n}_{(q,p;r)\omega}. \tag{83}$$

Substituting this into Eqs. (81) and (82), one observes that only integrals over momenta of these quantities are required:

$$\bar{Q}^{l,k;n,m}_{(p;q),\omega} = \int_s Q^{l,k;n,m}_{(p+s,s;q)\omega}, \quad \bar{K}^{k,m;l,n}_{(q;r)\omega} = \int_t K^{k,m;l,n}_{(t,q-t;r)\omega}. \tag{84}$$

These obey the following linear equations:

$$\bar{Q}^{l,k;n,m}_{(p;q),\omega} - \frac{gn}{2\pi}F^{lj,ik}_{p,\omega}\sigma_x^{i,g}\sigma_x^{h,j}\bar{Q}^{h,g;n,m}_{(p;q),\omega} = \frac{gn}{2\pi}F^{lj,ik}_{p,\omega}\sigma_x^{i,j}\sigma_x^{n,m}, \tag{85}$$

$$\bar{K}^{k,l;n,m}_{(p;r2)\omega} - \frac{gn}{2\pi}F^{k,g;l,h}_{p,\omega}\sigma_x^{h,i}\sigma_x^{g,j}\bar{K}^{i,j;n,m}_{(p;r2)\omega} = \frac{gn}{2\pi}F^{k,g;l,h}_{p,\omega}\sigma_x^{h,n}\sigma_x^{g,m}, \tag{86}$$

where the "fish" integrals

$$F^{k,l;m,n}_{p,\omega} = \frac{1}{\pi}\int_q G^{k,l}_{q,\omega}G^{m,n}_{p-q,\omega} \tag{87}$$

are similar to the "bubble" diagrams defined in Eq. (40). In the above formulas, only the summation over repeated matrix indices is assumed, whereas integrations over frequencies and momenta are all written explicitly.

As in Sec. III C, it is convenient to rescale the correlators like in Eq. (46) and momenta $\tilde{p}=(g/8\pi)^{-1/3}p$, since for these variables the response function ρ_ω depends on a single parameter n. The above rescaling leads to the same equations, Eqs. (85) and (86), with the following replacements: $\frac{gn}{2\pi}\to 4n$, $p\to\tilde{p}$, and $F^{k,i;m,n}_{p,\omega}\to f^{k,i;m,n}_{\tilde{p},\omega}=\frac{1}{\pi}\int_{\tilde{q}} g^{k,i}_{\tilde{q},\omega}g^{m,n}_{\tilde{p}-\tilde{q},\omega}$, with $g_{\tilde{q},\omega}=g_\omega+\sigma_x\tilde{q}^2$. Using an explicit dependence of the Green's functions on q (i.e., on the z component of the momentum), Eq. (38), it is easy to calculate all 16 components of $f^{k,i;m,n}_{p,\omega}$. Nonzero ones are listed in the Appendix.

Further using these expressions for the fish integrals we find an analytical solution for the linear chain equations, Eqs. (85) and (86), in terms of Green's functions derived above from the gap equation. Nonzero elements can also be found in the Appendix. Note that at criticality, i.e., for $a_T=a_T^g$, where $\rho_{\omega=0}=1/(2n)^{2/3}$, all the functions $\bar{K}$ and $\bar{Q}$ are singular at $\omega=p_z=0$. Having calculated the four-point correlator, we return now to the HLL contribution to current.

D. Lowest order non-Ohmic contribution to current

The expression for the current density Eq. (72) in terms of the partial derivatives calculated in the previous section reads

$$\sigma_{HLL} = \sigma_C + \sigma_D = \int_{\{\omega\nu;prqs\}} \delta_{p+q-r-s}\sigma_x^{k,l}\sigma_+^{m,n}G^{k,a}_{p,\omega}G^{m,b}_{q,\nu}G^{c,l}_{r,\omega}G^{d,n}_{s,\nu} \times \frac{\delta\mathcal{A}^{dis}_G}{\delta\bar{\Phi}^a_{p,\omega}\delta\bar{\Phi}^b_{q,\nu}\delta\bar{\Phi}^{*c}_{r,\omega}\delta\bar{\Phi}^{*d}_{s,\nu}}, \tag{88}$$

where the Cooperon and diffusion terms are given in terms of the chain functions:

$$\sigma_C = 4\pi n\left(\frac{8\pi}{g}\right)^{2/3}\int_{\omega\tilde{p}} \sigma_x^{a,b}\sigma_\uparrow^{c,d}\sigma_x^{j,k}\sigma_x^{j,l}f^{a,m;c,n}_{\tilde{p}}f^{i,b;j,d}_{\tilde{p}}\bar{K}^{k,l;m,n}_{\tilde{p},\omega},$$

$$\sigma_D = 4\pi n\left(\frac{8\pi}{g}\right)^{2/3}\int_{\omega\tilde{p}}(\sigma_x^{a,b}\sigma_\uparrow^{c,d}+\sigma_x^{c,b}\sigma_\uparrow^{a,d})$$
$$\times\sigma_x^{m,k}\sigma_x^{l,n}f_{\tilde{p}}^{c,n;m,b}f_{\tilde{p}}^{a,j;i,d}\bar{Q}_{\tilde{p},\omega}^{l,k;i,j}. \quad (89)$$

Integration over the z component of momentum was performed in a closed form. However, the result is rather bulky, and here, we present two asymptotic expressions only. As we observed in Sec. III, the LLL contribution to the current fails to account for the diverging resistivity on the glass line. Therefore we are mostly interested in the HLL "correction" near the glass line. The integral over ω in Eq. (89) is dominated by small frequencies. Let us first consider the correction right on the glass line. Using the relevant asymptotic expressions for solutions of the gap equation ρ_ω and c_ω given in Eq. (59), one obtains

$$\sigma_C = \sigma_D = \frac{\eta}{8}\left(\frac{4\pi}{rg}\right)^{1/2}\int_\omega \frac{1}{\omega^{5/4}}, \quad (90)$$

where $\eta=\frac{1}{\pi^2 2^{3/2}}\sqrt{\frac{\sqrt{2}-1}{6}}\approx 0.01$. One should emphasize that the integral diverges at the glass line, leading to an infinite conductivity on the glass line.

Near the glass line on the liquid side $a_T=a_T^g+\Delta_T$, the integral, although no longer divergent, is still dominated for small enough Δ_T by infrared. The integrand saturates at $\omega_{cut}\sim\omega_{\min}=\frac{1}{\tau_{rel}}$ when the frequency decreases with the relaxation time τ_{rel} given in Eq. (60). As a consequence, the conductivity diverges near the glass line as

$$\sigma_{HLL} = \frac{\eta}{(2n)^{5/6}}\left(\frac{8\pi}{g}\right)^{1/3}\frac{1}{\Delta^{1/2}}. \quad (91)$$

Assuming that parameters of the system (temperature and magnetic field) are on the static critical surface, we increase the electric field from zero to a small value $\Delta=bv^2$. Substituting Eq. (91) into the HLL contribution to the current, Eq. (76), one obtains near the glass transition

$$j_{HLL} = 2\eta\frac{(1+2v^2)}{\pi a_h^1 b^{1/2}}(2n)^{1/6}\left(\frac{g}{8\pi}\right)^{2/3}\frac{v}{|v|}. \quad (92)$$

This nonanalytic dependence is the main result of the present paper. Limits from positive and negative v at $v=0$ are constants of opposite signs due to the "friction" effect of disorder.

In the vortex glass phase, the dc conductivity is infinite throughout. The reason is that the response function $\rho_{\omega=0}$ is equal to its value at criticality everywhere, see Eq. (54). Therefore the diffusion and Cooperon chains have the same singularity at criticality, and the integral over ω diverges.

Above the static glass line in the unpinned phase, we still can write an approximate expression,

$$j_{HLL} = 2\eta\frac{(1+2v^2)}{\pi a_h^1}\frac{(2n)^{1/6}\left(\frac{g}{8\pi}\right)^{2/3}v}{\sqrt{2a_h^g-(1-t-b)+bv^2}},$$

which shows that far from the transition, the HLL current becomes Ohmic and gives a small correction to the dominant LLL contribution. Now we turn to phenomenological consequences of the analysis of previous sections.

V. IRREVERSIBILITY LINE, TIME CORRELATIONS, AND THE *I-V* CURVE

In this section, we provide expressions and discuss the dc conductivity and the nonlinear *I-V* curves as functions of both the material parameters (the coherence length, the penetration depth, anisotropy, T_c, the disorder strength, and the relaxation time) and the external parameters (magnetic and electric fields, temperature). We return to conventional notations.

We use the following basic units: length, ξ; time, $\tau_{GL}=\gamma\xi^2\simeq\frac{\hbar}{4T_c}$; energy, T_c; magnetic and electric fields, $H_{c2}(0)=\frac{\Phi_0}{2\pi\xi^2}$ and $E_0=\frac{4\hbar}{e^*\gamma\xi^3}\simeq\frac{16T_c}{e^*\xi}$, respectively; the current density, $J_0=\frac{4}{\sqrt{2}Gi}\frac{\gamma_a e^*}{\gamma\xi^4}$; and conductivity, $\sigma_0=\frac{E_0}{J_0}\simeq\frac{\sigma_n}{16(2\pi)^2}$, where σ_n is a normal state conductivity according to the clean case of BCS theory. Dimensionless material parameters characterizing the strength of thermal fluctuations, type-II property, anisotropy, and disorder are Gi, κ, $\gamma_a=\sqrt{\frac{m_c}{m^*}}$, and n_p, respectively. The last is proportional to the pinning site density and the strength of a pinning center.[2] The time scales are determined by the TDGL coefficient γ, which, according to the BCS based estimates, is twice the diffusion constant of the material.[26] Temperature and magnetic and electric fields are measured in the above units: $t=T/T_c$, $b=B/H_{c2}(0)$, and $\mathcal{E}=E/E_0$. We also make use of additional dimensionless parameters: the vortex velocity $v=\mathcal{E}b^{-3/2}$ and the disorder strength n_p. Sometimes we will also use temperature and field dependent functions: the mean field superfluid fraction $a_h=-\frac{1}{2}(1-t-b-\mathcal{E}^2/b^2)$, the LLL scaled temperature $a_T=2^{4/3}Gi^{-1/3}(bt)^{-2/3}a_h$, and the disorder parameter $n=\frac{a_h^2}{\pi\sqrt{2Git}}n_p$ characterizing the ratio between the disorder and the interaction strength.

A. Irreversibility line and correlations in the disordered vortex liquid

There are two homogeneous dynamical phases of the system in the three-dimensional external parameter space (T,H,J). The inhomogeneous phases were not considered in the present work and will be commented on in Sec. VI. The Fourier transform of the correlator of the order parameter ψ, as it appears in TDGL equations, Eqs. (1) and (3), is

$$\boldsymbol{C}(\omega)\equiv\int d\tau' e^{i\omega\tau'}\langle\psi(\mathbf{r},\tau+\tau')\psi^*(\mathbf{r},\tau')\rangle$$
$$=\frac{T_c m^*\gamma_a\tau_{GL}}{2\pi\hbar^2\xi}(tb)^{2/3}(2Gi)^{-1/6}\frac{c_\omega}{\rho_\omega^{1/2}+\rho_\omega^{*1/2}}. \quad (93)$$

An explicit LLL expression for dimensionless rescaled c_ω is given by Eq. (48) via response function of Eq. (47). A dynamical critical surface is defined as a set of values of the parameters for which the correlator $\boldsymbol{C}(\omega)$ diverges at $\omega\to 0$. One observes a pole in Eq. (48) when the response function ρ_ω approaches a constant $(2n)^{-2/3}$. This leads to the following

TABLE I. Critical exponents of the glass transition.

c_ω^g	c_0	τ_{rel}	σ_{HLL}	σ_{HLL}^g
$\omega^{-1/2}$	Δ^{-1}	Δ^{-2}	Δ^{-1}	$\omega^{-1/4}$

equation for the dynamic transition line [it is more convenient to use instead dimensionless scaled parameters $(t,b,\mathcal{E})$]:

$$\mathcal{E}_g^2/b^2 = 1 - t - b + 2a_h^g(t,b), \tag{94}$$

where

$$a_h^g(t,b) = \left[\frac{n_p(1-t)^2 b}{4\pi}\right]^{2/3}\left[\frac{3}{2} - \frac{4\pi t\sqrt{2Gi}}{n_p(1-t)^2}\right]. \tag{95}$$

The last term represents the effects of disorder, while the rest appear already on the mean field level.[4,16] In the static case, $\mathcal{E}=0$ and the glass line is given by the equation (see Fig. 2)

$$1 - t - b + 2a_h^g(t,b) = 0. \tag{96}$$

At small disorder, the line approaches the $b=0$ line and the glass phase disappears. In the opposite limit, the glass phase expands beyond the mean field normal-superconducting boundary $1-t-b=0$.

The dynamical correlator exposes the temporal relaxation of the order parameter due to an overall effect of dissipation, mesoscopic disorder, and thermal fluctuations. Asymptotically, the long time dependence of the correlator is exponential, $C(t-t') \propto \exp\left[-\frac{t-t'}{\tau_{rel}}\right]$. The singularity closest to the origin in the complex plane of the correlator c_ω determines the relaxation time [see Eq. (60)]

$$\frac{\tau_{rel}}{\tau_{GL}} = \frac{8}{3}Gi^{1/3}\frac{(bt)^{2/3}}{n^{4/3}\Delta^2}, \tag{97}$$

$$\Delta(t,b,\mathcal{E}) = 2a_h^g(t,b) - 1 + t + b + \mathcal{E}^2/b^2. \tag{98}$$

The correlator and the response function as functions of frequency are given in Fig. 1. The correlator decreases as $1/\omega^2$ at large frequencies. The relaxation time diverges as one approaches the critical surface determined next. Critical exponents are summarized in Table I.

The statics and the linear response within disordered GL model have been discussed in numerous theoretical, numerical, and experimental works. The glass line was first determined, to our knowledge, using the Martin-Siggia-Rose dynamical approach in Gaussian approximation[1] and was claimed to be obtained using resummation of diagram in Kubo formula in Ref. 23. Comparison with experiment on YBCO at relatively low field was made in Ref. 1 and that at very high magnetic fields (up to 50 T) was made in Ref. 16. It was found to be in a reasonably good agreement with the experiments. In the previous section, we extended the comparison to a low T_c strongly type-II superconductor $NbSe_2$. Other types of relatively strongly fluctuating type-II low T_c superconductors (like borocarbides[37]) exhibit similar glass line and the peak effect.

The glass transition line for the ΔT_c disorder was obtained using the replica formalism (within similar Gaussian approximation) by Lopatin,[15] and the result is identical to ours. This was generalized to other types of disorder (the mean free path disorder) in Ref. 16. The common wisdom is that the "replica" symmetry is generally broken in the glass (either via "steps" or via "hierarchical" continuous process) as in most of the spin glass theories.[25] The replica method applied to the static LLL model with the ΔT_c disorder within Gaussian approximation[16] indicates that there is no replica symmetry breaking in the homogeneous phase. However, the Edwards-Anderson parameter vanishes above the glass transition, while it is nonzero below it. This is in agreement with the original approach to the glass transition of Edwards and Anderson (see Ref. 38 for a discussion). The results obtained here demonstrate dynamical criticality in this case, in close analogy with the corresponding analysis in the spin glass theory.[20]

Finite electric fields (namely, transport beyond linear response) were also considered analytically in Ref. 21, and our result in the clean limit agrees with theirs. The elastic medium and the vortex dynamics within the London approximation were discussed beyond linear response in numerous analytic and numerical works. Although qualitatively the glass lines obtained here resemble the ones in phenomenological approaches based on comparison of disorder strength with thermal fluctuations and interaction,[39,40] the detailed form is different.

B. Relaxation of the order parameter in the vortex glass phase

In the glass phase, the Fourier transform of the correlator is

$$\boldsymbol{C}(\omega) = \frac{T_c m^* \gamma_a \tau_{GL}}{2\pi\hbar^2\xi(2Gi)^{1/2}}\left[\frac{\rho_\omega^* \rho_\omega}{\rho_\omega^{1/2} + \rho_\omega^{*1/2} - 4n\rho_\omega\rho_\omega^*} - \frac{\pi}{2}\Delta\delta(\omega)\right], \tag{99}$$

where ρ_ω is a solution of Eq. (67). In this phase, the electric field is zero and the value of a_T in this equation should be taken at $\mathcal{E}=0$. In addition to the DFT regular part, there is an additional contribution proportional to the Edwards-Anderson order parameter: $\frac{\pi}{2}\Delta$. It indeed approaches zero (linearly in Δ) near the glass transition surface. For small ω, the regular part of the correlator decreases as $\omega^{-1/2}$. In real space, they correspond to a constant (the persistent component[20]) and a powerwise decreasing component $\boldsymbol{C}(\tau) \propto (\tau/\tau_{GL})^{-1/2}$, respectively. The last is not critical and is very different from the time scale in the unpinned phase, τ_{rel}, which determines an *exponential* decay of the correlator. The long time scale response leads to irreversibility in the glass phase. Note here that we did not consider more general nonstationary solutions of the gap equations depending on two times $\boldsymbol{C}(\tau,\tau') = \langle\psi(\tau)\psi^*(\tau')\rangle$.

C. *I-V* curve and pinning force

In the unpinned (vortex liquid) phase, we obtain the following contributions to the supercurrent. The LLL part dominant above the glass line is

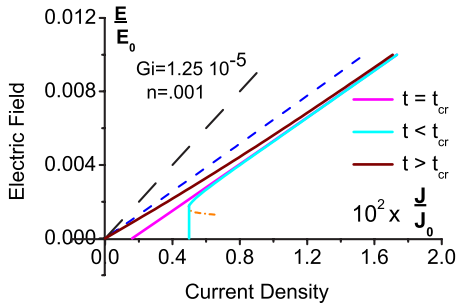

FIG. 3. (Color online) Typical *I-V* curves of the disordered superconductor above (the cyan line), on (the magenta line), and below (the blue line) the glass transition for $Gi=1.25\times10^{-5}$, $n=0.001$, and $b=0.2$. Above the glass line, $t>t_{cr}=0.683$, the *I-V* curve (the brown solid line) approaches the LLL result only (the blue dash line). On the glass line, $t=t_{cr}$, there appears a nonvanishing HLL contribution given by Eq. (102). In the glass phase, $t<t_{cr}$, the *I-V* curve becomes unstable (the dash-dotted red line) for current less than a critical value, Eq. (107), and electric field drops to zero value. The Bardeen-Stephen limit for a clean material is shown by a dashed line.

$$j_{LLL}=\frac{J_{LLL}}{J_0}=\frac{1}{2^{13/3}\pi}Gi^{1/3}\rho_0^{1/2}t^{2/3}b^{-1/3}\mathcal{E}, \tag{100}$$

where the dimensionless response function ρ_0 is given in Eq. (50) as a function of $a_T(t,b,\mathcal{E})$. Note the small numerical factor (consistent with the Bardeen-Stephen law, see below). The HLL contribution (containing the pinning force), dominant not very far from the static glass line, was calculated in Sec. IV:

$$j_{HLL}=\frac{J_{HLL}}{J_0}=f_H Gi^{3/4}\frac{n_p^{1/6}t^{3/2}(1-t)^{1/3}}{b^{1/3}\Delta^{1/2}}\mathcal{E}, \tag{101}$$

where the constant is $f_H=\frac{2^{3/4}}{\pi^{2/3}}\sqrt{\frac{\sqrt{2}-1}{3}}\approx0.29$. Upon approaching the static glass line, $\mathcal{E}\to0$ and $\Delta\to\mathcal{E}^2/b^2$. In this limit, j_{HLL} tends to a constant value, which is the depinning current:

$$j_{HLL}^g=f_H Gi^{3/4}n_p^{1/6}t^{3/2}(1-t)^{1/3}b^{2/3}, \tag{102}$$

while the LLL contribution vanishes, $j_{LLL}^g\simeq\frac{\mathcal{E}}{8(2\pi)^2}\frac{t(2Gi)^{1/3}}{(nbt)^{1/3}}\to0$. Note the low power of the disorder strength in this expression. This is in contrast to both single vortex and collective pinning models in the London limit, which have the $n_p^{2/3}$ dependence. Of course, we stress that our calculation is not done in the vortex solid phase. Since the homogeneous phase exists due to thermal fluctuation along with disorder, the dependence on the pinning strength is expected to be weaker.

In addition to the supercurrent, there are the normal electron's contribution to the current. It is contained in the GL free energy [not written explicitly in Eq. (3)] independent of the order parameter field. In the *I-V* curve in Fig. 3, the clean limit current,[2] $j_n=\frac{\mathcal{E}}{16(2\pi)^2}$, is shown by a dashed line.

D. Conductivity in the flux flow regime

Differential conductivity in units of σ_0 is obtained by differentiating the current in Eqs. (100) and (101) over the electric field:

$$\frac{dj_{LLL}}{d\mathcal{E}}=\frac{Gi^{1/3}}{2^{13/3}\pi^2}t^{2/3}b^{-1/3}\rho_0^{1/2}\times\left[1-\frac{1}{3Gi^{1/3}(2bt)^{2/3}(1-n)\rho_0^{1/2}+2a_h}\frac{\mathcal{E}}{b^2}\right], \tag{103}$$

$$\frac{dj_{HLL}}{d\mathcal{E}}=f_H Gi^{3/4}n_p^{1/6}t^{3/2}(1-t)^{1/3}b^{-1/3}\Delta^{-3/2}(2a_h^g-1+t+b), \tag{104}$$

where the nonlinear part was derived by differentiating the gap equation:

$$\frac{d\rho_0^{1/2}}{d\mathcal{E}}=-\frac{\rho_0^{1/2}}{3Gi^{1/3}(2bt)^{2/3}(1-n)\rho_0^{1/2}+2a_h}\frac{\mathcal{E}}{b^2}.$$

Function $\rho_0(a_T)$ is given explicitly in Eq. (50), while the constant a_h^g can be found in Eq. (95). One observes that the LLL contribution has a small positive nonlinear part. There is a weak singularity (due to the appearance of the persistent part in the correlator) on the glass line, but it remains finite and continuous in the glass phase. On the other hand, the HLL part is infinite inside the glass phase, and therefore, electric fields cannot penetrate.

Conductivity is obtained in the limit $\mathcal{E}\to0$:

$$\frac{\sigma_{LLL}}{\sigma_0}=\frac{Gi^{1/3}}{2^{13/3}\pi^2}t^{2/3}b^{-1/3}\rho_0^{1/2}, \tag{105}$$

$$\frac{\sigma_{HLL}}{\sigma_0}=f_H Gi^{3/4}\frac{n_p^{1/6}(1-t)^{1/3}t^{3/2}}{b^{1/3}}(2a_h^g-1+t+b)^{-1/2}. \tag{106}$$

Near the glass line, the HLL contribution to conductivity diverges as $\Delta^{-1/2}$ [the deviation from criticality parameter Δ was defined in Eq. (98)] due to HLL part. However, above the glass transition (where the nonlinear corrections are generally small), the HLL contribution decreases rapidly and the LLL contribution takes over. In the clean limit $n_p\to0$ (no disorder on the mesoscopic scale), the last one transforms into the Bardeen-Stephen law:[32] $\sigma=\frac{1}{16(2\pi)^2}\frac{1-t-b}{b}$.

The divergence of conductivity on the glass line that we obtained in Sec. IV was assumed in Ref. 1 and linked phenomenologically to the general scaling theory of the vortex glass proposed in Ref. 5. The divergence was claimed to be derived on the basis of the calculation of the higher order diagrams in Ref. 41, however, this seems doubtful to us due to the fact that an important imaginary (the relaxation) part in the basic propagator G_0 was omitted. We were unable to reproduce their glass lines or the flux flow resistivity even in the liquid phase.

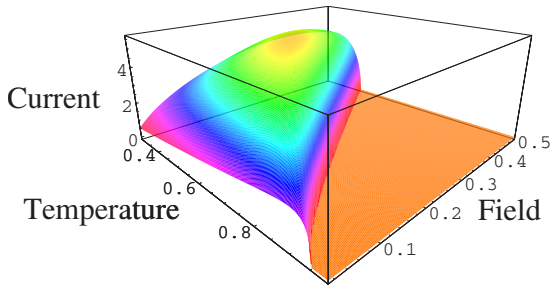

FIG. 4. (Color online) The J-b-t diagram of the critical current at $Gi=1.25\times10^{-5}$ and $n=0.01$. The critical current (in arbitrary units) is equal to zero above the static glass line.

In the extreme case, when the current is large enough, the system is depinned. We discuss now the critical current in both the homogeneous and crystalline vortex phases, and discuss the theory of the so-called peak effect in critical current.

VI. THEORY OF THE DISCONTINUOUS PEAK EFFECT

Critical current is one of the most important characteristics of the superconducting materials. It has been known for a long time that in magnetic fields, the critical current rather counterintuitively rises when the field (or temperature) approaches $H_{c2}(T)$.[42] The phenomenon was linked early on to softening of the vortex lattice and its eventual melting. We, therefore, start with the critical current in the homogeneous phase in the presence of mesoscopic thermal fluctuations.

A. Critical current in the uniform amorphous (vortex glass) state and the dynamical phase diagram

The vortices are pinned in the regions below the dynamical glass line on T-H phase diagram, and the conductivity is infinite. However, at a sufficiently large current j, the vortices become mobile and the vortex system jumps from superconducting state into a dissipative Ohmic state, with the nonzero electric field inside. The transition occurs when, for a given temperature t and magnetic field b, the electric field $\mathcal{E}$ approaches the value on the dynamical glass line given by Eq. (94). The critical current at which the system depins is obtained from Eqs. (100) and (101) for $\mathcal{E}=\mathcal{E}_g$, in which case $\rho_0=(2n)^{-2/3}$,

$$j_{LLL}^{cr}(t,b)=\frac{J_{LLL}^{cr}}{J_0}=\frac{2^{1/6}}{2^4\pi^{2/3}}Gi^{1/2}n_p^{-1/3}tb^{2/3}(1-t)^{-2/3}\times[1-t-b+2a_h^g(t,b)]^{1/2},$$

$$j_{HLL}^{cr}(t,b)=f_HGi^{3/4}n_p^{1/6}t^{3/2}(1-t)^{1/3}b^{2/3}\times[1-t-b+2a_h^g(t,b)]^{-1/2}. \quad (107)$$

The current is proportional to the "pinning force." This dynamical transition surface is shown in Fig. 4 for $Gi=1.25\times10^{-5}$ and $n=0.01$. The line separating liquid and glass phases is similar to the static glass line (except for the small magnetic field region), but it lies below the last one.

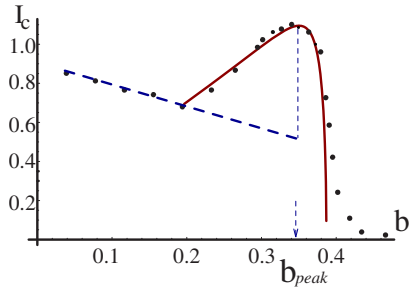

FIG. 5. (Color online) Magnetic field dependence of the critical current in the vortex glass phase (solid line) and in the vortex crystalline phase (the dash line) in comparison with data on $NbSe_2$ at $T=4.2$ K obtained using the mode locking transport technique (Ref. 43) (points). Dynamical melting occurs at $B^{peak}=b_{peak}H_{c2}$. Below that point, the data follow a metastable amorphous state.

As will be discussed next, one cannot use the formulas presented here below the dynamical melting line (at low temperatures and fields), where the vortex matter is not homogeneous.

B. Inhomogeneous phases

We did not consider crystalline disordered phases or dynamical melting line[43] in this work (although the line was discussed in statics in Refs. 27 and 44). Nevertheless, one can use the expression for the critical current, Eq. (107), and for the glass line, Eq. (96), to qualitatively discuss the peak effect, namely, a maximum of the critical current (estimated typically from magnetization measurements) observed both in low[42] and high[45] T_c materials. Typically in low T_c materials, both the melting line and the glass line lie in the vicinity of the mean field normal-superconductor line; see Fig. 2 for $NbSe_2$.

We fit the irreversibility line using the measurements of Banerjee *et al.*[36] in the inset of Fig. 2. The parameters used are the dimensionless pinning strength, defined in Eq. (4), $n_p=1.2\times10^{-3}$, and the Ginzburg parameter $Gi=5\times10^{-8}$. The value of Gi differs from that used in many papers (Refs. 29, 36, and 46, and references therein), however, notice that their definition of Gi is different. Using the obtained parameters, one can estimate the critical current in the homogeneous phase according to Eq. (107) (solid line in Fig. 5). The normalization factor was chosen from the best fit. Above the intersection point, one observes the peak effect. Following Ref. 47, we phenomenologically estimate the crystalline phase critical current using the elasticity theory[48] (dashed line in Fig. 5), while in the homogeneous amorphous phase our result is used.

This description of the peak effect is qualitatively different from the traditional one. The conventional explanation, originally due to Pippard,[47,49] invokes a gradual "softening" of the vortex lattice when the temperature approaches melting. At the melting point, the critical current jumps to zero (in practice, it might be smeared out by sample inhomogeneities).

The present view, supported by recent experiments in which Corbino geometry or width dependence were used to

minimize or subtract the edge effects,[13,14,46] attributes the peak to the amorphous homogeneous state. Critical current actually jumps from a relatively low value in the crystalline state to a very high value in the vortex glass. Qualitatively, this is due to the fact that it is easier to pin a disordered homogeneous state than a rigid crystalline one. The continuous rise of the critical current observed in numerous earlier experiments (see Refs. 43 and 47 as examples) was caused by poor resolution due to overheating of the solid and overcooling of the homogeneous states. It was argued theoretically[50] that the supercooled liquid state exists and has energy very close to the crystalline state. Experimentally, it was convincingly shown[51] that the states for fields below B^{peak} in Fig. 5 are metastable. Consequently, the system in the experiment of Ref. 43 follows the crystalline critical current (dashed line in Fig. 5) until it intersects the amorphous line (solid line). Our expression for the critical current in the amorphous phase describes well the overcooled amorphous state when the crystalline state is energetically favorable, see Fig. 5. For $B > B^{peak}$, the crystalline state becomes metastable and the critical current, Eq. (107), rapidly drops (as $\sqrt{T-T^g}$, namely, with classical critical exponent) when temperature approaches the glass temperature T^g. To summarize, the traditional picture predicts a gradual increase with subsequent drop of the critical current, while our picture predicts a sudden increase followed by a fast but continuous decrease. It would be important to further clarify experimentally which picture is the correct one.

Of course, the very notion of the critical current should be carefully defined due to the appearance of creep at elevated temperatures.[52] We comment on this and other related questions next.

VII. CONCLUSIONS

We start from brief comments on several loosely related theoretical and phenomenological issues.

The strict vortex glass hypothesis[5] assumes that, even at finite temperatures, electric field does not penetrate the true vortex glass phase. This is an idealization at a nonzero temperature since thermal fluctuations generate the vortex creep.[52] In spite of the fact that the Gaussian approximation used in the present work is a nonperturbative method, it has limitations. The effects of creep are not seen, very much like in the renormalized perturbation theory. The creep appears as (exponentially small) "instantons" contributions, which correspond to tunneling events of a single vortex. These effects can be incorporated into the present discussion in a straightforward manner.[2] Therefore the critical current, strictly speaking, vanishes at nonzero temperatures; however, the I-V curve exhibits a well defined crossover behavior[53] (rounding of the curve in Fig. 3).

It was noted in Sec. IV that *the LLL contribution* to conductivity is proportional to the superfluid density $\rho=|\psi|^2$ due to an identity $\mathbf{J} \propto \hat{\mathbf{z}} \times \nabla \rho$. On the other hand, it is generally known that magnetization, even beyond LLL (and to leading order in very small parameter $1/\kappa^2$), is also proportional to $|\psi|^2$.[3,21,54] Phenomenologically, the behavior of the two quantities near the glass transition line is very different. This was considered to be a difficulty for the LLL approach to type-II superconductivity in strong magnetic field. Here, we showed explicitly what happens. The vortex pinning force responsible for divergence of conductivity is solely due to the higher Landau level contribution, for which the above identity does not hold. Consequently, the proportionality between conductivity and the superfluid density is also violated.

Therefore, away from the glass line, the two quantities have the LLL scaling as was demonstrated, for example, by several experiments on YBCO for both magnetization[55] and conductivity,[56] while near the glass line (experimentally determined in Ref. 57), the scaling is violated. Correspondingly, the static correlator $\boldsymbol{C}(t=t')=\frac{1}{2\pi}\int_\omega C_\omega$ (proportional to the magnetization within LLL) does not diverge at the critical surface, while the persistent part of the dynamical correlator $C_{\omega=0}$ does, see Eq. (99), and stays infinite throughout the glass phase. Thus the former cannot serve as an order parameter for the "glass" transition, even in the static limit. In our calculation, the magnetization is continuous across the glass line but has a jump in derivative with respect to temperature or other external parameters. This behavior was observed in BSCCO using the "shaking" technique.[27]

The discussion can be easily generalized to incorporate the Hall current as in Ref. 32 by including the nondissipative (Gross-Pitaevsky) term $i\frac{\hbar^2\gamma_H}{4m^*}D_\tau\psi$ in the TDGL equation, Eq. (1), and to the 2D case. The generalization to essentially layered material via Lawrence-Doniach model is much more complicated. We did not attempt to study the ac transport or relaxation. This is quite possible and many experimental results require such a generalization. For an excellent example of the ac current-voltage characteristics, see Ref. 58. Moreover, the formalism presented in this work allows, in principle, consideration of various time dependent phenomena characteristic of a glass state: irreversibility, memory,…. For this one will have to drop the assumption of stationarity, within which the correlator and the response function depend only on the difference of two times, $\boldsymbol{C}(t,t') \neq \boldsymbol{C}(t-t')$.

The theory can also be generalized to the 2D case appropriate for description of thin films or strongly layered superconductors and compared to experiments. The comparison for organic superconductor κ type BEDT−TTF (Ref. 59) and BSCCO (Ref. 27) of the static glass line is quite satisfactory. There exist, to our knowledge, just two Monte Carlo simulations of the disordered GL model,[60,61] both in 2D, in which no clear irreversibility line was found. However, the frustrated XY model was recently extensively simulated[7,8] including the glass transition line and I-V curves. It shares many common features with the GL model although disorder is introduced in a different way, so that it is difficult to compare the dependence of pinning. The I-V curves and the glass line resemble our results. We plan to calculate the helicity modulus and the structure factor, on which authors concentrate in most of these works.

To conclude, we quantitatively described the competition between interactions, thermal fluctuations, and random quenched disorder using the dynamical Martin-Siggia-Rose approach to the Ginzburg-Landau model of the vortex matter. Within the Gaussian approximation, we characterized the transition between pinned and unpinned vortex matter. The

location of the glass transition line between the homogeneous phases was determined and compared to experiments. The dynamic correlation and response functions of the order parameter in homogeneous phases were found. This enables one to estimate the relaxation properties of the vortex matter due to the combined effect of pinning and thermal fluctuation. It was shown that in the glass phase the correlator has a persistent component, vanishing on the glass line. The relaxation time in the vortex liquid was calculated. By extending the theory beyond the linear response, the non-Ohmic *I-V* curves were found and the analytical expression for the critical current in both electric and magnetic fields was determined. The critical current as a function of field, temperature, and disorder strength was calculated and compared with recent experiments. A quantitative theory of the peak effect has been proposed.

ACKNOWLEDGMENTS

We are grateful to G. Bel, D. P. Li, E. H. Brandt, T. Maniv, G. Menon, E. M. A. Dorsey, X. Hu, P. J. Lin, T. J. Yang, A. Koshelev, E. Zeldov, and especially to V. Vinokur for discussions; to P. H. Kes, N. Kokubo, E. Andrei, and A. Grover for discussion and sending results prior to publication; and to R. Ikeda for explaining his work. This work was supported by the NSC of the R.O.C. (No. 952112M009048) and the MOE ATU Program.

APPENDIX: COOPERON AND DIFFUSION CHAIN INTEGRALS

Nonzero components of the "fish" integrals $f^{k,i1;m,i2}_{\tilde{p},\omega} = \frac{1}{\pi}\int_{\tilde{q}} g^{k,i1}_{\tilde{q},\omega} g^{m,i2}_{\tilde{p}-\tilde{q},\omega}$ are given by

$$f^{11;11}_{\tilde{p},\omega} = \frac{8(\rho_\omega + 3|\rho_\omega| + \rho^\star_\omega) + 2\rho_\omega\rho^\star_\omega\tilde{p}^2}{(\rho^{1/2}_\omega + \rho^{*1/2}_\omega)(4+\rho_\omega\tilde{p}^2)(4+\rho^\star_\omega\tilde{p}^2)(\rho_\omega + 2|\rho_\omega| + \rho^\star_\omega + \rho_\omega\rho^\star_\omega\tilde{p}^2)} c^2_\omega,$$

$$f^{11;12}_{p,\omega} = (f^{11;21}_{p,\omega})^* = f^{12;11}_{p,\omega} = (f^{21;11}_{p,\omega})^* = \frac{6|\rho_\omega| + 4\rho^\star_\omega + 2\rho_\omega + \rho_\omega\rho^\star_\omega\tilde{p}^2}{(\rho^{1/2}_\omega + \rho^{*1/2}_\omega)(4+\rho_\omega p^2)(\rho_\omega + 2|\rho_\omega| + \rho^\star_\omega + \rho_\omega\rho^\star_\omega\tilde{p}^2)} \times \rho_\omega c_\omega,$$

$$f^{12;21}_{p,\omega} = f^{21;12}_{p,\omega} = \frac{\rho_\omega\rho^\star_\omega(\rho^{1/2}_\omega + \rho^{*1/2}_\omega)}{(\rho_\omega + 2|\rho_\omega| + \rho^\star_\omega + \rho_\omega\rho^\star_\omega\tilde{p}^2)},$$

$$f^{12;12}_{p,\omega} = (f^{21;21}_{p,\omega})^* = \frac{\rho^{3/2}_\omega}{(4+\rho_\omega\tilde{p}^2)}.$$

The integrals have been used to solve the linear "chain equations" [Eqs. (85) and (86)]. Below we list explicitly nonzero components of the solution

$$\bar{Q}^{11;12}_{\bar{p},\omega} = \bar{Q}^{11;21}_{\bar{p},\omega} = \frac{8nc_\omega[4(\rho_\omega\rho^*_\omega)^{1/2} + 4(\rho_\omega + \rho^*_\omega) + \rho_\omega\rho^*_\omega\tilde{p}^2]}{(\rho^{1/2}_\omega + \rho^{*1/2}_\omega)Y_{\omega\bar{p}}Y^*_{\omega\bar{p}}},$$

$$\bar{Q}^{12;12}_{\bar{p},\omega} = \bar{Q}^{12;21}_{\bar{p},\omega} = (\bar{Q}^{21;12}_{\bar{p},\omega})^* = (\bar{Q}^{21;21}_{\bar{p},\omega})^* = \frac{8n\rho^{3/2}_\omega}{Y_{\omega\bar{p}}}, \quad \text{(A1)}$$

$$\bar{K}^{11;12}_{\bar{p},\omega} = \bar{K}^{11;21}_{\bar{p},\omega} = \frac{4nc_\omega\rho_\omega[6(\rho_\omega\rho^*_\omega)^{1/2} + 2\rho_\omega + 4\rho^*_\omega + \rho_\omega\rho^*_\omega\tilde{p}^2]}{(\rho^{1/2}_\omega + \rho^{*1/2}_\omega)Y_{\omega\bar{p}}X_{\omega\bar{p}}}, \quad \text{(A2)}$$

$$\bar{K}^{12;12}_{\bar{p},\omega} = \bar{K}^{21;21}_{\bar{p},\omega} = \frac{16n^2(\rho_\omega\rho^*_\omega)^2(\rho^{1/2}_\omega + \rho^{*1/2}_\omega)^2}{[(\rho^{1/2}_\omega + \rho^{*1/2}_\omega)(\rho^{1/2}_\omega + \rho^{*1/2}_\omega + 4n\rho_\omega\rho^*_\omega) + \rho_\omega\rho^*_\omega\tilde{p}^2]X_{\omega\bar{p}}},$$

$$\bar{K}^{21;21}_{\bar{p},\omega} = \bar{K}^{21;21}_{\bar{p},\omega} = \frac{4n(\rho_\omega\rho^*_\omega)(\rho^{1/2}_\omega + \rho^{*1/2}_\omega)[(\rho^{1/2}_\omega + \rho^{*1/2}_\omega)^2 + \rho_\omega\rho^*_\omega\tilde{p}^2]}{[(\rho^{1/2}_\omega + \rho^{*1/2}_\omega)(\rho^{1/2}_\omega + \rho^{*1/2}_\omega + 4n\rho_\omega\rho^*_\omega) + \rho_\omega\rho^*_\omega\tilde{p}^2]X_{\omega\bar{p}}},$$

$$\bar{K}^{11;22}_{\bar{p},\omega} = \frac{4nc_\omega[Z_\omega + (4\rho_\omega\rho^*_\omega + \rho^{*1/2}_\omega + \rho^{1/2}_\omega)\rho_\omega\rho^*_\omega\tilde{p}^2]}{(\rho^{1/2}_\omega + \rho^{*1/2}_\omega)^2 Y_{\omega\bar{p}}Y^*_{\omega\bar{p}}X_{\omega\bar{p}}},$$

$$\bar{K}^{11;11}_{\bar{p},\omega} = (\bar{K}^{22;22}_{\bar{p},\omega})^* = \frac{8n\rho^{3/2}_\omega}{Y_{\omega\bar{p}}},$$

$$\bar{K}^{12;22}_{\bar{p},\omega} = \bar{K}^{21;22}_{\bar{p},\omega} = -\frac{4nc_\omega\rho^*_\omega(6\rho^{1/2}_\omega\rho^{*1/2}_\omega + 4\rho_\omega + 2\rho^*_\omega + \rho_\omega\rho^*_\omega\tilde{p}^2)}{(\rho^{1/2}_\omega + \rho^{*1/2}_\omega)Y^*_{\omega\bar{p}}X_{\omega\bar{p}}},$$

where $Z_\omega = 4(\rho^{*3/2}_\omega + \rho^{3/2}_\omega + 4\rho_\omega\rho^{*1/2}_\omega + 4\rho^{1/2}_\omega\rho^*_\omega) + 16n\rho_\omega\rho^*_\omega(\rho^{1/2}_\omega + \rho^{*1/2}_\omega)^2$ and

$$X_{\omega\bar{p}} = (\rho^{1/2}_\omega + \rho^{*1/2}_\omega)(\rho^{1/2}_\omega + \rho^{*1/2}_\omega - 4n\rho_\omega\rho^*_\omega) + \rho_\omega\rho^*_\omega\tilde{p}^2,$$

$$Y_{\omega\bar{p}} = (4 - 8n\rho^{3/2}_\omega + \rho_\omega\tilde{p}^2). \quad \text{(A3)}$$

At criticality $a_T = a^g_T$, where $\rho_{\omega=0} = 1/(2n)^{2/3}$, all the functions $\bar{K}$ and $\bar{Q}$ are singular at $\omega = p_z = 0$.

[1] A. T. Dorsey, M. Huang, and M. P. A. Fisher, Phys. Rev. B **45**, 523 (1992).
[2] G. Blatter, M. V. Feigel'man, V. B. Geshkenbein, A. I. Larkin, and V. M. Vinokur, Rev. Mod. Phys. **66**, 1125 (1994).
[3] D. J. Thouless, Phys. Rev. Lett. **34**, 946 (1975); E. Brezin, D. R. Nelson, and A. Thiaville, Phys. Rev. B **31**, 7124 (1985).
[4] R. S. Thompson and C. R. Hu, Phys. Rev. Lett. **27**, 1352 (1971).
[5] M. P. A. Fisher, Phys. Rev. Lett. **62**, 1415 (1989); D. S. Fisher, M. P. A. Fisher, and D. A. Huse, Phys. Rev. B **43**, 130 (1991).
[6] T. Nattermann, Phys. Rev. Lett. **64**, 2454 (1990); T. Natterman and S. Scheindl, Adv. Phys. **49**, 607 (2000).
[7] C. J. Olson and C. Reichhardt, Phys. Rev. B **61**, R3811 (2000); Y. Nonomura and X. Hu, Phys. Rev. Lett. **86**, 5140 (2001); P. Olsson and S. Teitel, *ibid.* **87**, 137001 (2001); Q. H. Chen and X. Hu, *ibid.* **90**, 117005 (2003); A. D. Hernandez and D. Dominguez, *ibid.* **92**, 117002 (2004).
[8] P. Olsson, Phys. Rev. Lett. **98**, 097001 (2007).
[9] H. S. Bokil and A. P. Young, Phys. Rev. Lett. **74**, 3021 (1995).
[10] T. Giamarchi and P. Le Doussal, Phys. Rev. Lett. **75**, 3372 (1994); **76**, 3408 (1996); Phys. Rev. B **52**, 1242 (1995); P. Le Doussal and T. Giamarchi, *ibid.* **57**, 11356 (1998).
[11] S. E. Korshunov, Phys. Rev. B **48**, 3969 (1993).
[12] A. van Otterlo, R. T. Scalettar, and G. T. Zimanyi, Phys. Rev. Lett. **81**, 1497 (1998); C. Reichhardt, A. van Otterlo, and G. T. Zimanyi, *ibid.* **84**, 1994 (2000).
[13] Y. Paltiel *et al.*, Phys. Rev. Lett. **85**, 3712 (2000); Y. Paltiel *et al.*, Nature (London) **403**, 398 (2000).
[14] Z. L. Xiao, E. Y. Andrei, Y. Paltiel, E. Zeldov, P. Shuk, and M. Greenblatt, Phys. Rev. B **65**, 094511 (2002).
[15] A. V. Lopatin, Europhys. Lett. **51**, 635 (2000).
[16] D. Li, B. Rosenstein, and V. Vinokur, J. Supercon. Novel Magnet. **19**, 369 (2006).
[17] Z. Tesanovic and I. F. Herbut, Phys. Rev. B **50**, 10389 (1994).
[18] A. I. Larkin and A. A. Varlamov, in *Handbook on Superconductivity: Conventional and Unconventional Superconductors*, edited by K. H. Bennemann and J. B. Ketterson (Springer, New York, 2002).
[19] P. C. Martin, E. D. Siggia, and H. A. Rose, Phys. Rev. A **8**, 423 (1973).
[20] H. Sompolinsky and A. Zippelius, Phys. Rev. B **25**, 6860 (1982).
[21] T. Blum and M. A. Moore, Phys. Rev. B **56**, 372 (1997).
[22] G. F. Mazenko, *Nonequilibrium Statistical Mechanics* (Wiley-VCH, Weinheim, 2006).
[23] A. Ikeda, T. Ohmi, and T. Tsuneto, J. Phys. Soc. Jpn. **59**, 1740 (1990); **61**, 254 (1992); A. Ikeda, *ibid.* **64**, 1683 (1994); **64**, 3925 (1995).
[24] D. Li, A. M. Malkin, and B. Rosenstein, Phys. Rev. B **70**, 214529 (2004).
[25] K. H. Fischer and J. A. Hertz, *Spin Glasses* (Cambridge University Press, New York, 1991); V. Dotsenko, *An Introduction to the Theory of Spin Glasses and Neural Networks* (Cambridge University Press, Cambridge, 2001).
[26] J. B. Ketterson and S. N. Song, *Superconductivity* (Cambridge University Press, Cambridge, 1999); M. Tinkham, *Introduction to Superconductivity* (McGraw-Hill, New York, 1996).
[27] H. Beidenkopf, N. Avraham, Y. Myasoedov, H. Shtrikman, E. Zeldov, B. Rosenstein, E. H. Brandt, and T. Tamegai, Phys. Rev. Lett. **95**, 257004 (2005).
[28] D. T. Fuchs, E. Zeldov, T. Tamegai, S. Ooi, M. Rappaport, and H. Shtrikman, Phys. Rev. Lett. **80**, 4971 (1998).
[29] A. Pautrat, J. Scola, Ch. Simon, P. Mathieu, A. Brulet, C. Goupil, M. J. Higgins, and S. Bhattacharya, Phys. Rev. B **71**, 064517 (2005).
[30] A. Kovner and B. Rosenstein, Phys. Rev. D **39**, 2332 (1989).
[31] H. Kleinert, *Path Integrals in Quantum Mechanics, Statistics, and Polymer Physics* (World Scientific, Singapore, 1995).
[32] R. J. Troy and A. T. Dorsey, Phys. Rev. B **47**, 2715 (1993).
[33] We make use of a ghost field slightly different from the field used by Sompolinsky: $\phi = i\phi_{Somp}$.
[34] C. De Dominicis and L. Peliti, Phys. Rev. B **18**, 353 (1978).
[35] J. M. Cornwall, R. Jackiw, and E. Tomboulis, Phys. Rev. D **10**, 2428 (1974).
[36] S. S. Banerjee *et al.*, Physica C **355**, 39 (2001).
[37] M.-O. Mun, S.-I. Lee, W. C. Lee, P. C. Canfield, B. K. Cho, and D. C. Johnston, Phys. Rev. Lett. **76**, 2790 (1996); D. Jawal-Nagar, A. D. Thakur, M. R. Eskildsen, P. C. Canfield, S. M. Yusuf, S. Ramakrishnan, and A. K. Grover, Physica B **359-361**, 476 (2005).
[38] J.-P. Bouchaud and A. Georges, Phys. Rep. **195**, 127 (1990).
[39] Y. Radzyner, A. Shaulov, and Y. Yeshurun, Phys. Rev. B **65**, 100513(R) (2002); Y. Radzyner, A. Shaulov, Y. Yeshurun, I. Felner, K. Kishio, and J. Shimoyama, *ibid.* **65**, 100503(R) (2002).
[40] G. P. Mikitik and E. H. Brandt, Phys. Rev. B **64**, 184514 (2001); G. I. Menon, *ibid.* **65**, 104527 (2002).
[41] R. Ikeda, J. Phys. Soc. Jpn. **65**, 3998 (1996).
[42] W. DeSorbo, Rev. Mod. Phys. **36**, 90 (1964); P. H. Kes and C. C. Tsuei, Phys. Rev. B **28**, 5126 (1983); M. Menghini, Y. Fasano, and F. de la Cruz, *ibid.* **65**, 064510 (2002).
[43] N. Kokubo, R. Besseling, and P. H. Kes, Phys. Rev. B **69**, 064504 (2004); N. Kokubo, K. Kadowaki, and K. Takita, Phys. Rev. Lett. **95**, 177005 (2005); N. Kokubo, T. Asada, K. Kadowaki, K. Takita, T. G. Sorop, and P. H. Kes, Phys. Rev. B **75**, 184512 (2007).
[44] D. Li and B. Rosenstein, Phys. Rev. B **65**, 220504(R) (2002).
[45] W. K. Kwok, J. A. Fendrich, C. J. van der Beek, and G. W. Crabtree, Phys. Rev. Lett. **73**, 2614 (1994); S. Sarkar, D. Pal, P. L. Paulose, S. Ramakrishnan, A. K. Grover, C. V. Tomy, D. Dasgupta, B. K. Sarma, G. Balakrishnan, and D. McK. Paul, Phys. Rev. B **64**, 144510 (2001).
[46] S. S. Banerjee *et al.*, Phys. Rev. B **62**, 11838 (2000); O. Dogru, E. Y. Andrei, M. J. Higgins, and S. Bhattacharya, Phys. Rev. Lett. **95**, 057004 (2005).
[47] C. Tang, X. Ling, S. Bhattacharya, and P. M. Chaikin, Europhys. Lett. **35**, 597 (1996).
[48] E. H. Brandt, Rep. Prog. Phys. **58**, 1465 (1995), and references therein.
[49] A. B. Pippard, Philos. Mag. **19**, 217 (1969); A. I. Larkin and Yu. N. Ovchinnikov, J. Low Temp. Phys. **34**, 409 (1978).
[50] D. Li and B. Rosenstein, Phys. Rev. Lett. **90**, 167004 (2003); Phys. Rev. B **70**, 144521 (2004).
[51] Z. L. Xiao, E. Y. Andrei, and M. J. Higgins, Phys. Rev. Lett. **83**, 1664 (1999).
[52] P. Le Doussal and V. M. Vinokur, Physica C **254**, 63 (1995).
[53] A. I. Larkin, M. C. Marchetti, and V. M. Vinokur, Phys. Rev. Lett. **75**, 2992 (1995).
[54] Z. Tešanović, L. Xing, L. Bulaevskii, Q. Li, and M. Suenaga, Phys. Rev. Lett. **69**, 3563 (1992).
[55] S. Salem-Sugui, M. Friesen, A. D. Alvarenga, F. G. Gandra, M. M. Doria, and O. F. Schilling, Phys. Rev. B **66**, 134521 (2002).

[56] A. Wahl, V. Hardy, F. Warmont, A. Maignan, M. P. Delamare, and Ch. Simon, Phys. Rev. B **55**, 3929 (1997).
[57] Y. Ando *et al.*, Phys. Rev. B **60**, 12475 (1999); R. Gilardi, S. Streule, N. Momono, M. Oda, and J. Mesot, Eur. Phys. J. B **47**, 231 (2005).
[58] Y. Paltiel, Y. Myasoedov, E. Zeldov, G. Jung, M. L. Rappaport, D. E. Feldman, M. J. Higgins, and S. Bhattacharya, Phys. Rev. B **66**, 060503(R) (2002).
[59] G. Bel, D. P. Li, B. Rosenstein, V. Vinokur, and V. Zhuravlev, Physica C, doi:10.1016/j.physc.2007.04.169 (2007).
[60] A. K. Kienappel and M. A. Moore, Phys. Rev. B **56**, 8313 (1997).
[61] M. S. Li and T. Nattermann, Phys. Rev. B **67**, 184520 (2003).